AD_____

GRANT NUMBER: DAMD17-94-J-4477

TITLE: Molecular Genetics of Breast Neoplasia

PRINCIPAL INVESTIGATOR: David C. Ward, Ph.D.

CONTRACTING ORGANIZATION: Yale University School of Medicine
New Haven, CT 06520-8047

REPORT DATE: October 1996

TYPE OF REPORT: Annual

PREPARED FOR: Commander
U.S. Army Medical Research and Materiel Command
Fort Detrick, Frederick, MD 21702-5012

DISTRIBUTION STATEMENT: Approved for public release;
distribution unlimited

The views, opinions and/or findings contained in this report are those of the author(s) and should not be construed as an official Department of the Army position, policy or decision unless so designated by other documentation.

DTIC QUALITY INSPECTED 3

19970605 120

REPORT DOCUMENTATION PAGE

Form Approved
OMB No. 0704-0188

Public reporting burden for this collection of information is estimated to average 1 hour per response, including the time for reviewing instructions, searching existing data sources, gathering and maintaining the data needed, and completing and reviewing the collection of information. Send comments regarding this burden estimate or any other aspect of this collection of information, including suggestions for reducing this burden, to Washington Headquarters Services, Directorate for Information Operations and Reports, 1215 Jefferson Davis Highway, Suite 1204, Arlington, VA 22202-4302, and to the Office of Management and Budget, Paperwork Reduction Project (0704-0188), Washington, DC 20503.

1. AGENCY USE ONLY *(Leave blank)*	2. REPORT DATE	3. REPORT TYPE AND DATES COVERED
	October 1996	Annual (29 Sep 95 - 28 Sep 96)

4. TITLE AND SUBTITLE
Molecular Genetics of Breast Neoplasia

5. FUNDING NUMBERS
DAMD17-94-J-4477

6. AUTHOR(S)
David C. Ward, Ph.D.

7. PERFORMING ORGANIZATION NAME(S) AND ADDRESS(ES)
Yale University School of Medicine
New Haven, CT 06520-8047

8. PERFORMING ORGANIZATION REPORT NUMBER

9. SPONSORING/MONITORING AGENCY NAME(S) AND ADDRESS(ES)
Commander
U.S. Army Medical Research and Materiel Command
Fort Detrick, MD 21702-5012

10. SPONSORING/MONITORING AGENCY REPORT NUMBER

11. SUPPLEMENTARY NOTES

12a. DISTRIBUTION / AVAILABILITY STATEMENT
Approved for public release; distribution unlimited

12b. DISTRIBUTION CODE

13. ABSTRACT *(Maximum 200*

The overall objective of this grant is to develop new multiparametric fluorescence *in situ* hybridization (M-FISH) techniques for the analysis of chromosomal abnormalities and genetic alterations in breast carcinoma cells and tissues. During year 02, we continued to refine and validate the M-FISH procedure for karyotyping metaphase chromosomes in which each chromosome is identified by a unique spectral signature that is generated by simultaneous hybridization of 24 differentially labeled chromosome specific "painting" probes. Both simple and highly complex chromosomal aberrations can be detected readily by M-FISH. Extenstion of M-FISH to fresh or paraffin-embedded tissues is in progress and is largely focused on the development of novel software that combines z-axis optical sectioning, image deconvolution, 3-D image reconstruction and spectra signature extraction. We have also completed an analysis of 27 primary breast carcinoma samples for abnormalities in mRNA transcribed from the FHIT (fragile histidine triad) gene, a candidate tumor suppressor gene mapped to the 3p14 region of the genome. Aberrant FHIT RNAs were detected in 40% of the tumors examined, suggesting that the FHIT gene may be involved in the progression of a subset of breast carcinomas.

14. SUBJECT TERMS
Breast Cancer, cancer cell karyotyping, fluorescence in situ hybridization, abnormal expression of the FHIT gene.

15. NUMBER OF PAGES
44

16. PRICE CODE

17. SECURITY CLASSIFICATION OF REPORT	18. SECURITY CLASSIFICATION OF THIS PAGE	19. SECURITY CLASSIFICATION OF ABSTRACT	20. LIMITATION OF ABSTRACT
Unclassified	Unclassified	Unclassified	Unlimited

NSN 7540-01-280-5500

Standard Form 298 (Rev. 2-89)
Prescribed by ANSI Std. Z39-18
298-102

FOREWORD

Opinions, interpretations, conclusions and recommendations are those of the author and are not necessarily endorsed by the U.S. Army.

____ Where copyrighted material is quoted, permission has been obtained to use such material.

____ Where material from documents designated for limited distribution is quoted, permission has been obtained to use the material.

____ Citations of commercial organizations and trade names in this report do not constitute an official Department of Army endorsement or approval of the products or services of these organizations.

____ In conducting research using animals, the investigator(s) adhered to the "Guide for the Care and Use of Laboratory Animals," prepared by the Committee on Care and use of Laboratory Animals of the Institute of Laboratory Resources, national Research Council (NIH Publication No. 86-23, Revised 1985).

____ For the protection of human subjects, the investigator(s) adhered to policies of applicable Federal Law 45 CFR 46.

____ In conducting research utilizing recombinant DNA technology, the investigator(s) adhered to current guidelines promulgated by the National Institutes of Health.

____ In the conduct of research utilizing recombinant DNA, the investigator(s) adhered to the NIH Guidelines for Research Involving Recombinant DNA Molecules.

____ In the conduct of research involving hazardous organisms, the investigator(s) adhered to the CDC-NIH Guide for Biosafety in Microbiological and Biomedical Laboratories.

David C Ward 12/28/96

PI - Signature Date

TABLE OF CONTENTS

Front Cover	1
Report Documentation (SF298)	2
Table of Contents	4
Introduction	5
Progress Report (Body)	6-12
Conclusions	12-13
References	13-15
Appendices:	16
A) Tables and Figures with Legends	17-20
B) 3 papers reporting research supported by this grant (DAMD-17-4477):	

1. Speicher, M.R., Ballard, S.G., and Ward, D.C. "Karyotyping human chromosomes by combinatorial multicolor FISH." Nat. Genet, 2:368-375 (1996).

2. Speicher, M.R., Ward, D.C. "The coloring of cytogenetics." Nature Medicine, 2(9):1046-1048 (1996).

3. Speicher, M.R., Ballard, S.G. and Ward, D.C. "Computer image analysis of combinatorial multi-fluor FISH (in press)

INTRODUCTION

The development of breast cancer, as well as other neoplasias, is thought to occur by cumulative alterations in the genome, possibly acquired in an orderly fashion. These changes appear to be responsible for the passage of the disease through hyperplastic, benign, malignant, and metastatic stages of growth. Some genetic alterations are found in a variety of tumor types, while others appear to be involved in tumor tissue specificity. In breast cancer, recurrent genomic changes reportedly have been associated with many chromosomal locations and involved both amplifications and deletions of chromosomal segments as well as translocation breakpoints. However, only a few specific genes within these regions have been identified and characterized at the molecular level. P53, RB-1, BRCA-1, BRCA-2, and cathepsin D mutations and deletions have been found to predispose individuals towards malignancy (1). Furthermore, overexpression of the c-erb B-2/Her-2/neu oncogene has been found in a significant number of breast tumors (2). The functions that these genes play in regulating the normal cell cycle and the mechanisms by which their disruption leads to neoplasia are not well understood. Knowledge of genetic changes occurring during the inception and progression of tumorigenesis is necessary for the development of new diagnostic markers and therapies, rational analysis of treatment protocols, tracking remission progression, and assessing genetic risk status.

The overall objective of this project is to develop new fluorescence *in situ* hybridization (FISH) techniques that would permit the analysis of multiple genetic loci simultaneously in breast tumor tissues, in chromosomes prepared from short term cultures of breast tumor cells or in tumor cell lines. Specifically, we propose to develop chromosome "painting" probe sets that can be combinatorially labeled with different fluorescent dyes such that karyotype analysis of tumor cell chromosomes is feasible using multicolor FISH (M-FISH). In addition, we propose to establish probe sets for specific genes and chromosomal regions implicated in the pathophysiology of breast carcinoma and to develop experimental protocols for multiplex FISH analysis of such probes in fresh or paraffin-embedded tissues. Finally, we propose to study the role of genes mapping in the p14-21 region of chromosome 3 in the initiation, progression or metastasis of breast cancer. These objectives constitute the four tasks reported in the Statement of Work (Section G) of our original grant proposal. The following report below outlines the progress made during the year 02 period.

PROGRESS REPORT

1) Further Development of M-FISH Chromosome Analysis

During the first year of support all our efforts were focused on the identification of appropriate sets of fluorophores and optical filter sets that would permit the spectral resolution of 7 fluors simultaneously and the utilization of chromosomal DNA painting libraries, combinatorially labeled with these fluors, to carry out 24 color M-FISH karyotyping. These initial studies were documented in the year 01 Progress Report. A significant portion of year 02 has been devoted to validating the utility of M-FISH by analyzing, in a blind fashion, multiple cell lines previously subjected to conventional karyotyping. These studies have included a variety of breast carcinomas, ovarian carcinomas, squamous cell carcinomas of the head and neck, leukemias, lymphomas as well as numerous normal cell samples. While the M-FISH data show a high degree of concordance with conventional cytogenetics (>95%) there are some limitations that need to be addressed. The technical aspects of M-FISH, the types of data obtained to date and the relative merits and pitfalls of M-FISH are detailed in the three publications appended to this years report. These publications unequivocally demonstrate our ability to detect both simple and complex karyotypic changes by M-FISH, many of which could not be defined by conventional cytogenetics, and establish M-FISH as a useful adjunct for further defining chromosomal abnormalities in tumor cells detected using comparative genome hybridization.

One of the major limitations of the M-FISH procedure is the requirement to add a large excess (10-20 fold) of Cot-1 DNA to the painting probe mixture in order to suppress cross-hybridization of the repetitive DNA sequences present in each of the chromosomal libraries that constitute the painting probes. The Cot-1 DNA not only increases the complexity (and viscosity) of the probe cocktail, it also represents the most expensive component of the hybridization mixture (>90%). We have, therefore, begun to systematically subtract Cot-1 DNA sequences from each of the microdissected chromosome libraries. We are using a procedure that was recently shown by Dr. Thomas Cremer (Munich) to be highly effective in removing this family of repetitive sequences (T. Cremer, personal communication). Briefly, the stock microdissected chromosome-specific libraries are amplified by polymerase chain reaction (PCR) using degenerate oligonucleotide primers (3). Cot-1 DNA is biotinylated chemically using a commercially available photoactivatable agent (Boehringer Mannheim). The chromosome-specific libary PCR product is denatured and hybridized to single-stranded biotinylated Cot-1 DNA. The hybrids are captured and removed using streptavidin coated magnetic beads. The supernatant fraction, now partially depleted of repetitive sequences, is reamplifed by PCR. After several cycles of subtraction, the residual chromosomal DNA in the supernatant fraction should be depleted sufficiently of

Cot-1 DNA hybridizable sequences so that hybridization done without addition of competing Cot-1 DNA shows no evidence of crosshybridization. This can be easily established by FISH as incomplete subtraction results in cross-hybridization to all chromosomes in the metaphase spread. All 24 libraries need to be subtracted fully only once, thus, Cot-1 DNA-free painting probes can be generated for subsequent use by PCR. Depletion of the libraries should also markedly reduce the hybridization times required for M-FISH because of the lower genetic complexity of the probe mix.

A second significant limitation of M-FISH is that it provides no chromosomal banding data for the identification of chromosomal subregions. Thus, certain types of chromosome rearrangements, such as pericentric inversions, are not detectable by the current version of M-FISH nor can chromosomal translocations be assigned to specific cytogenetic bands. To circumvent this problem, we have worked on identifying a filter set that would enable us to discriminate yet another fluorophore (Cy1, Cascade blue or Lucifer yellow) when incorporated into the existing fluorophore set. This has now been accomplished and we are currently testing Cascade blue labeled Alu sequence oligonucleotides to generate R-banding profiles that can be added to the M-FISH data representation. Additional software refinements have been undertaken to make this feasible. Our ultimate goal is to present M-FISH results as similarly to conventional cytogenetics as possible; ie., black and white (or gray scale) ideograms (in which chromosome identification is based on the spectral signature provided by the combinatorially labeled chromosome painting probe) containing standard G-banding data (produced by inverting the R-banding images produced by hybridization of the Alu-oligomer labeled with Cascade blue).

During year 02, we have also initiated M-FISH studies using normal and tumor cell lines cultured *in vitro*. These studies are a prelude to applying M-FISH to fresh frozen or paraffin-embedded tissue sections. Development of this technology, using either painting probes or specific sets of genes will be much more difficult and complex than chromosome karyotyping. Since the interphase nucleus has considerable 3-D structure relative to metaphase chromosome spreads, it will be necessary to do Z-axis optical sectioning, image deconvolution and 3-D image reconstruction in addition to extracting spectra signature data. Sophisticated competer algorithms are needed to achieve this objective and efforts to develop such software were initiated during year 02. These studies, which involve collaborative interactions with Drs. Thomas Cremer, Peter Lichter, David Agard and their colleagues in Munich, Heidelberg and San Francisco, respectively, will continue during year 03 of the project. The development of this software will be necessary before meaningful evaluation of M-FISH using cultured cells and tissue section material can be undertaken.

2) Analysis of the Expression of the FHIT gene in Breast Carcinomas

One of the stated tasks in Section G of our grant proposal was to investigate the possible role in breast carcinomas of genes mapping in the 3p14-21 region of the genome. Many molecular and cytogenetic studies have indicated that the 3p14-21 area may harbor one or more putative tumor supressor genes important in the progression of breast carcinoma (4) (5), lung cancers (6), renal cell carcinoma (7), cervical carcinoma (8), as well as thyroid (9), and head and neck cancers (10). Recently a candidate gene has been isolated that appears to span the t(3;8) translocation in familial renal cell carcinoma and the 3p14.2 fragile site (11). This gene, designated FHIT (fragile histidine triad), is a member of the histidine triad family of enzymes and has been found to be highly conserved over evolution sharing 60-70% homology with a gene found in Schizosaccharomyces pombe (diadenosine 5',5'''-P^1,P^4-tetraphosphate (Ap4) asymmetrical hydrolase) which cleaves the Ap4A substrate asymmetrically into ATP and AMP. FHIT expression abnormalities were originally described in digestive tract tumors (esophagus, stomach, and colon). Alterations in the genome and its expression have also been observed in lung cancer (12), and more recently in breast cancer cell lines, as well as some primary breast tumors (13), and head and neck tumors (14).

The intriguing initial studies on FHIT abnormalities prompted us to examine the expression of the FHIT gene in 27 primary breast tumors, predominantly of the intraductal and invasive type. We used both reverse transcriptase-polymerase chain reaction (RT-PCR) and RNase mismatch cleavage (RMC) assays, coupled with DNA sequencing, to determine if deletions or insertions occurred in FHIT transcripts isolated from these breast tumors. Our data, summarized below, indicate that between 15 and 40% of the tumors examined have aberrant FHIT RNAs, suggesting that the FHIT gene may be involved in the progression of at least a subset of breast tumors.

2.1) Results

We analyzed RNA from the 27 primary breast tumors described in Table 1. Primary tumors were sectioned by microtome after H&E staining keeping normal tissue to a minimum. Use of primers 5U1 and 3D1 (see Material and Method Section below) resulted in the amplification of a small portion of the 5' untranslated region and essentially all of the coding region (exons 3 through 9 and a portion of exon 10) in 26 of the 27 cases. As an internal control and to assess RNA quality, a 289 bp fragment from the human Beta actin gene was routinely amplified using the same PCR reaction mixtures and PCR conditions. Full length fragment was obtained in a reproducible manner when doing RT-PCR using RNA prepared from normal human peripheral blood lymphocytes. Four of 27 cases screened (BC-D, BC-3, BC-7, and BC-13; see Table 1 and Figure I) amplified both full length FHIT

fragment and deletion products. In one case (BC-16, Fig.1b) all amplification products were clearly or slightly larger than wild type, indicating insertions. The presence of at least two mismatched bases was confirmed in BC-16 by RNase digestion (see below). Occasionally low levels of transcripts clearly longer than the normal FHIT transcript were seen (BC-10 and BC-13) (Fig 1b); however, these were not tabulated as insertions into transcripts because they were not observed consistantly. Since amplification of the FHIT fragment from BC-15 RNA yielded wild type length fragment without larger or smaller fragments in the same experiment, stringency was considered sufficient. The small amplification product obtained in case BC-D was sequenced and found to lack exons 5,6, 7, and 8. Multiple base substitutions also were present (data not shown). BC-D DNA was used directly as template with exon 3, 4 and 5 specific primers. In two experiments all three primers failed to amplify specific fragments. However, appropriate exon fragments 3, 4 and 5 were amplified when using DNA from two othe primary breast tumors (BC-A and BC-B) in which the FHIT transcripts appear to be normal.

Aberrant FHIT transcripts were found by both RT-PCR and mismatch analysis in four cases: BC-D, BC-3, BC-7 and BC-16 (Table 1 and Fig. 2). A deletion transcript was detected by RT-PCR in case BC-13 using primer sets 5U1 & 3D1 and T7-5U1 & SP6-3D1 (Fig.1b), however, a small fragment was not detected by mismatch analysis (Fig.2). In general, fragments under 400 bp were not detected using the RNase digestion assay. A 100 bp DNA ladder (Gibco BRL) treated in the same manner as test and control amplification products also could only be visualized at approximately 400 bp (Fig. 2). The Mismatch Detect II kit while not having the sensitivity to pick up small deletion transcripts clearly had the ability to distinguish one or two basepair mismatches in the full length FHIT fragment from abnormal tissue (Fig. 2).

Controls were used to verify the different steps of mismatch analysis. Nested primers supplied by Ambion that amplified a 781 bp fragment from wild type and mutant p53 codons 111-371 were hybridized using all possible permutations of sense and antisense transcripts and promoters. After digestion with the RNase solutions (I, II, and III) supplied with the kit, expected cleavage patterns were observed (data not shown). Wild type FHIT fragment from normal peripheral blood was routinely used as control along side test samples (Fig. 2). To check promoter efficacy as well as polymerase activity, T7 and SP6 transcription reactions were carried out in the same tube using wild type p53 as template. After hybridization, aliquots of this reaction mixture were digested with RNase solutions I, II, and III. Titration experiments also were done to show that all reactions contained approximately equal RNA concentrations. Non- isotopic mismatch analysis is a qualitative assay, however success depends on similar levels of RNA synthesis of the two strands generated for hybridization. Empirically, the T7 promoter seemed a stronger promoter than

SP6 when transcribing mutant templates, so the SP6 promoter was routinely used to generate wild type FHIT antisense strand.

In six out of twenty-seven cases analyzed by mismatch analysis, a full length RT-PCR transcript appeared to have one or more mismatch basepairs detectable by at least one of the three RNase solutions supplied with the Ambion kit. These mismatches were confirmed by DNA sequencing, thus ruling out cleavages due to possible polymorphism. Collectively, the data obtained by RT-PCR and RNase Digestion assays indicate that as many as eleven out of twenty-seven primary breast tumors screened (40% of total cases) may have had aberrant FHIT transcripts. However, only four cases were found to have aberrant transcripts by both methodologies. In one case we found evidence of anomaly by RT-PCR alone, in six cases we found evidence of aberration in transcripts by mismatch analysis alone. Since the sensitivities of the two assays may differ significantly and no definitive correlations of the two methods with well characterized tumor samples have yet been done, we conservatively estimate that FHIT gene expression is abnormal in at least 15% of the cases screened but maybe as much as 40%.

The presence of aberrant FHIT transcripts did not correlate with a particular TNM classification, tumor stage or tumor size (Table 1). Four of eight tumors of T1 classification were positive for FHIT transcription anomalies (50%); Four of fourteen T2 tumors were positive (29%), two of three T3 tumors (66%) and one of two T4 tumors were positive (50%). The node status of twenty-two of the twenty-seven patients screened also was assessed. Nine of the patients screened had no metastatic homolateral axillary nodes (No). Twelve of the patients screened had movable homolateral axillary metastatic nodes, not fixed to one another or other structures (N1), one patient had nodes that were fixed to one another or other structures (N2). Four of the No group were positive for FHIT expression anomalies (44%), five of the N1 group were FHIT positive (41%); the other two positive FHIT cases were not assessed. One case with N2 status was not positive for FHIT expression anomalies. In most cases the distant metastases were not assessed. Three cases designated M1 were not positive for FHIT aberrant expression. Staging based on TNM classification showed three out of six Stage I tumors positive for aberrant FHIT expression (50%), five out of fourteen Stage II (36%), two out of two stage III (100%), and one out of five stage IV (20%). Nuclear grouping led to the finding that 55% of positive cases were in Nuclear group II, 27% of the cases were in Nuclear group III, 18% of the cases were not assessed. In Histological grouping 27% of the cases were in group II, 55% of the cases in group III, and 18% were not assessed.

Estrogen and progesterone receptor status and flow cytometry reports were available for nine of the eleven cases positive for aberrant FHIT transcription. Eight out of these nine cases (89%) were either estrogen or progesterone receptor negative (five were estrogen and progesterone receptor negative, one estrogen receptor negative and progesterone receptor positive, two were estrogen receptor positive and progesterone receptor negative). Six out of

these nine cases (67%) had parameters from flow cytometric studies indicating predominantly adverse prognoses. Additional cases need to be evaluated before definitive clinical correlations, if any, can be established.

2.2) Materials and Methods

RNA EXTRACTION AND REVERSE TRANSCRIPTION

Total and poly(A+) mRNA was extracted from breast tumor tissue using TRIzol Reagent (Gibco BRL). Fresh tumor specimens were frozen immediately after excision and stored at either -70^{0}C or in liquid nitrogen prior to RNA extraction. Samples were sectioned by microtome and judged to be between 70-99% tumor cells by hematoxylin and eosine (H&E) staining. Several sections cut by microtome immediately following the section used for H&E analysis were used for RNA preparation with TRIzol. After isolation the RNA was solubilized in RNase free water, 20-40 Units of RNAsin (Promega) was added prior to storage at -70^0 C. Reverse transcription was performed in 20 ml final volume containing 20mM Tris-HCL (pH 8.4), 50mM Kcl, 5mM $MgCl_2$, 10mM DTT, 1mM dNTPs, 500 ng oligo(dT) or 5mM random hexamer, 200 units SUPERSCRIPT II (Life Technologies Inc., Gaithersburg, MD), and 5mg of RNA. Primers and RNA were incubated at 70^{0}C for ten minutes and then chilled on ice. After addition of buffer, DTT, dNTPs, and MMLV-RT reactions were incubated at room temperature for ten minutes, and then at 42^{0}C for sixty minutes. MMLV-RT enzyme was inactivated at 70^{0}C for fifteen minutes prior to using the first strand synthesis for PCR amplification.

PCR AMPLIFICATION

The design of oligonucleotides used for generating RT-PCR products has been previously described (11). Two microliters of first strand synthesis was used for first round PCR amplification with a final volume of 100 ml. Primers 5U2 and 3D2 were used at a concentration of 0.8mM in 1X PCR buffer, 1.5mM $MgCl_2$, 200mM dNTPs and 1.25 Units Taq polymerase (Perkin Elmer Cetus). Reaction conditions consisted of one cycle of denaturation at 95^{0}C for 3 minutes, thirty cycles of 94^{0}C for 20 seconds, 60^{0}C for 30 seconds, 72^{0}C for 1 minute, and a final extension at 72^{0}C for 5 minutes using a Perkin Elmer Cetus PCR thermocycler model 9600. Two microliters of the amplified product was used directly for a second round of PCR using nested primers 5U1 and 3D1 (8). The cycling conditions for second round PCR were the same as first round PCR described above. As an internal control for each case, b actin primers (5' GGT CAC CCA CAC TGT GCC CAT CTA

CG 3' and 5' GGA TGC CAC AGG ACT CCA TGC CCA G 3') were used to amplify a 289bp fragment of the human b actin gene. In a limited number of cases the genome was screened directly using primers that amplify exons 3, 4, and 5 of the FHIT gene. These primers have been described elsewhere (8). The primers used for the RNase digestion assay were designed to incorporate T7 and SP6 phage promoters onto 5U1 and 3D1 respectively (T7-5U1: 5' TAA TAC GAC TCA CTA TAG GGT AGT GCT ATC TAC ATC 3' and SP6-3D1: 5' ATT TAG GTG ACA CTA TAG GAT GAT TCA GTT CCT CTT GG 3'). The PCR products were resolved on a ethidium bromide stained 0.8% agarose gel (SeaKem LE).

RNase DIGESTION ASSAY

A Mismatch Detect II kit was purchased from Ambion. The procedure outlined in the kit is an adaptation of Myers et al. (15) and Winter et al.(16). The method works on the principle that mismatches in RNA hybrids may be cleaved by RNase A. Briefly, RT-PCR is performed as described above. Phage promotors T7 and SP6 are incorporated into the second pair of nested primers (T7-5U1 and SP6-3D1). After transcribing the PCR product the single stranded test "sense" RNA was hybridized to single stranded wild type "antisense" RNA. The duplexes were digested with three proprietary RNase solutions as described in the kit. The products were visualized by gel electrophoresis in 2% high resolution agarose (Ambion). Wild type and mutant p53 primers were supplied in the kit as controls. The wild type FHIT PCR fragments generated by nested primers was sequenced prior to use.

CONCLUSIONS

1) We have successfully developed a novel method for karyotyping chromosomes based on the selective discrimination of chromosome specific hybridization probe sets using multicolor fluorescence. Comparison with conventional cytogenetics indicates that M-FISH offers specific advantages for the analysis of complex karyotypes and thus of significant potential utility for cancer cytogenetics. Incorporation of banding probes and full automation of the imaging system is expected to occur within the next 12 months. This will complete one of the goals in our work plan.

2) Application of M-FISH to cells and tissues is much more complex due to the fact that 3-D image analysis will be required. It is anticipated that development of the prerequisite software will occupy the major part of the efforts in the next 12 months. Demonstration of M-FISH on cellular specimens will not likely be done until early 1998.

3) The FHIT gene appears to be altered in a significant fraction of the primary breast carcinoma cases we have examined resulting in transcripts which are either larger or smaller

than the FHIT transcript produced by normal tissue. Additional cases need to be examined. The transcriptional profile patterns also need to be carefully correlated with other clinical and biochemical data prior to making any conclusions on the biological significance of the FHIT gene in breast tumorigenesis.

4) During the third (and final) year of support we plan on implementing a fully automated M-FISH karyotyping system and test it in our clinical genetics laboratory. We will initiate interphase M-FISH as soon as the prerequisite software is developed. Meanwhile, we will assemble cDNA and genomic DNA clones for the known oncogenes, tumor supressor genes, and other genetic loci implicated in the pathophysiology of breast carcinoma. cDNA clones will also be used to construct gridded arrays on glass slides so that gene expression profiles of breast carcinoma cells also can be established by quantitative ratio imaging. Gene expression profiling studies will be used to replace the proposed interphase M-FISH experiments should software development fall behind schedule.

REFERENCES

1. Sato, T. Akiyama, F., Sakamoto, G., Kasumi, F. and Nakamura, Y. A cumulation of genetic alterations and progression of primary breast cancer. Cancer Res., 51:5794-5799 (1995)

2. Tiwari, R.K., Borgen, P.I., Wong, G.Y., Cordon-Cardo, C., Osborne, M.P. HER-2/neu amplification and overexpression in primary human breast cancer is associated with early metastasis. Anticancer Research 12(2):419-25, 1992.

3. Craig, J.M., Kraus, J. and Cremer, T. Removeal of repetitive sequences from FISH probes using PCR-assisted affinity chromatography. Genomics (1997) in press.

4. Devilee,P., van den Broek, M., Kuipers-Dijkshoorn, N., Kolluri, R., Khan, P.M., Pearson, P.L., Cornelisse, C.J. At least four different chromosomal regions are involved in loss of heterozygosity in human breast carcinoma. Genomics, 5:554-560 (1989).

5. Pandis, N., Jin, Y., Limon, J., Bardi, G., Idvall, I., Mandahl, N., Mitelman, F., Heim, S. Interstitial deletion of the short arm of chromosome 3 as a primary chromosome abnormality in carcinomas of the breast. Genes, Chromosomes , and Cancer 6(3):151-155 (1993).

6. Naylor, S.L., Johnson, B.E., Minna, J.D., Sakaguchi, A.Y. Loss of heterozygosity of chromosome 3p markers in small-cell lung cancer. Nature 329 (6138): 451-454 (1987).

7. Kovacs, G., Erlandsson, R., Boldog, F., Ingvarsson, S., Muller-Brechlin, R., Klein, G., Sumegi, J. Consistent chromosome 3p deletion and loss of heterozygosity in renal cell carcinoma. Proc. Natl. Acad. Sci., USA 85(5):1571-1575 (1988).

8. Yokota, J., Tsukada, Y., Nakajima, T., Gotoh, M., Shimosato, Y., Mori, N., Tsunokawa, Y., Sugimura, T., Terada, M. Loss of heterozygosity on the short arm of chromosome 3 in carcinoma of the uterine cervix. Cancer Res. 49(13):3598-3601 (1989).

9. Herrmann, M.A., Hay, I.D., Bartelt, D.H. Jr., Ritland, S.R., Dahl, R.J., Grant, C.S, Jenkins, R.B. Cytogenetic and molecular genetic studies of follicular and papillary thyroid cancers. J. Clin. Invest. 88(5):1596-1604 (1991).

10. Latif, F., Fivash, M., Glenn, G., Tory, K., Orcutt, M.L., Hampsch, K., Delisio, J., Lerman, M., Cowan, J., Beckett, M., Weichselbaum, R. Chromosome 3p deletions in head and neck carcinomas: statistical ascertainment of allelic loss. Cancer Res. 52(6):1451-1456 (1992).

11. Ohta, M., Inoue, H., Cotticelli, M.G., Kastury, K., Baffa, R., Palazzo, J., Siprashvili, Z., Mori, M., McCue, P., Druck, T., Croce, C.M., Huebner, K. The FHIT gene, spanning the chromosome 3p14.2 fragile site and renal carcinoma-associated t(3;8) breakpoint, is abnormal in digestive tract cancers. Cell 84(4):587-597 (1996).

12. Sozzi, G., Veronese, M.L., Negrini, M., Baffa, R.,Cotticelli, M.G., Inoue, H., Tornielli, S., Pilotti, S., De Gregorio, L., Pastorino, U., Pierotti, M.A., Ohta, M., Huebner, K., Croce, C.M. The FHIT gene at 3p14.2 is abnormal in lung cancer. Cell 85(1):17-26 (1996).

13. Negrini, M., Monaco, C., Vorechovsky, I., Ohta, M., Druck, T., Baffa, R., Huebner, K., Croce, C.M. The FHIT gene at 3p14.2 is abnormal in breast carcinomas. Cancer Res. 56: 3173-3179 (1996).

14. Virgilio, L., Shuster, M., Gollin, S.M., Veronese, M.L., Ohta, M., Huebner, K., Croce, C.M. FHIT gene alterations in head and neck squamous cell carcinomas. Proc. Natl. Acad. Sci. USA 93: 9770-9775 (1996).

15. Myers, R.M., Larin, Z., Maniatis, T. Detection of single base substitutions by ribonuclease cleavage at mismatches in RNA:DNA duplexes. Science 230(4731):1242-1246 (1985).

16. Winter, E., Yamamoto, F., Almoguera, C., Perucho, M. A method to detect and characterize point mutations in transcribed genes. Proc. Nat. Acad. Sci. USA 82:7575-7579 (1985).

APPENDICES

1. Figures, Figure Legends and Table references in the body of the Progress Report.

2. Three manuscripts (2 published, 1 in press) describing research supported by this grant.

FIGURE LEGENDS

Fig. 1. Detection of Abberant FHIT Transcripts in Primary Breast Tumors by RT-PCR Amplification. RNA was extracted using TRIzol reagent (Gibco-Brl) and reverse transcribed. PCR products, made as described in Materials and Methods, were separated on 0.8% agarose gel by electrophoresis.

a.) Lane 1: 1 kb marker (Gibco-Brl); lanes 2&3: blank; FHIT PCR products amplified from normal peripheral blood using 5U1 and 3D1 primers (lane 4); amplification from primary breast tumor BC-A using 5U1 &3D1 primers (lane 5); BC-B and primers 5U1 & 3D1 (lane 6); BC-C and primers 5U1 and 3D1 (lane 7); BC-D and primers 5U1 and 3D1 (lane 8); blank (lane 9); b-actin PCR products amplified from normal peripheral blood (lane 10); BC-A and b-actin primers (lane 11), BC-B and b-actin primers (lane 12), BC-C and b-actin primers (lane 13), BC-D and b-actin primers (lane 14).

b.) Lane 1: 1 kb marker (Gibco-Brl); lane 2: amplification of 500 bp fragment of Lambda phage genome (7131-7630) as positive control; lane 3: negative control; lanes 4-7 (a): 5U1 & 3D1 primers and BC10, BC13, BC15, BC16 as template; lanes 8-11: (b) T7-5U1 & SP6-3D1 primers and BC10, BC13, BC15, BC16 as template; lanes 12-15 (c): b actin primers and BC10, BC13, BC15, BC16 as template.

Fig. 2. Detection of Aberrant FHIT Transcripts in Primary Breast Tumors by Non-isotopic RNase Digestion Assay (See Materials and Methods). Phage promoters T7 and SP6 were incorporated into the 5U1 and 3D1 primers specific for FHIT. After transcription of the FHIT PCR product, single stranded test "sense" RNA was hybridized to single stranded wild type "antisense" RNA. Aliquots of each duplex were digested with RNase solutions I, II, & III as supplied with the commercial kit. Lane 1: 100 bp marker (Gibco-Brl); lanes 2-4: case BC10 RNase solutions I, II, III; lanes 5-7: case BC13 RNase solutions I, II, III; lanes 8-10: case BC15 RNase solutions I, II, III; lanes 11-13: case BC16 RNase solutions I, II, III; lanes 14-16: case BC7 RNase solutions I, II, III; lanes 17-19: case BC8 RNase solutions I, II, III; lanes 20-22: Wild Type FHIT control RNase solutions I, II, III.

A

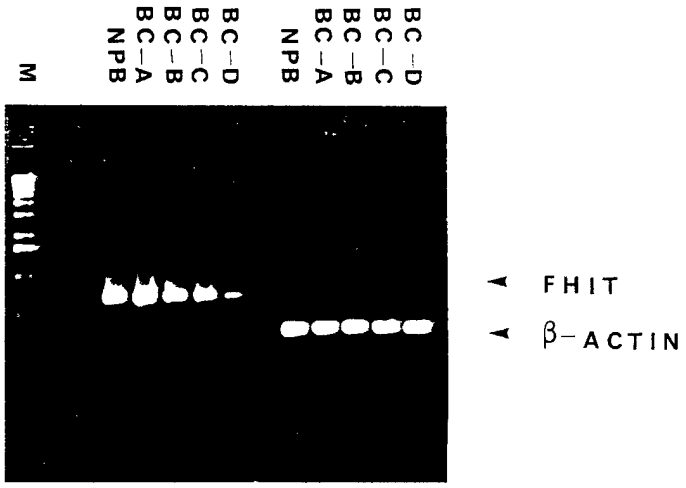
M
NPB
BC—A
BC—B
BC—C
BC—D
NPB
BC—A
BC—B
BC—C
BC—D
FHIT
β-ACTIN

B

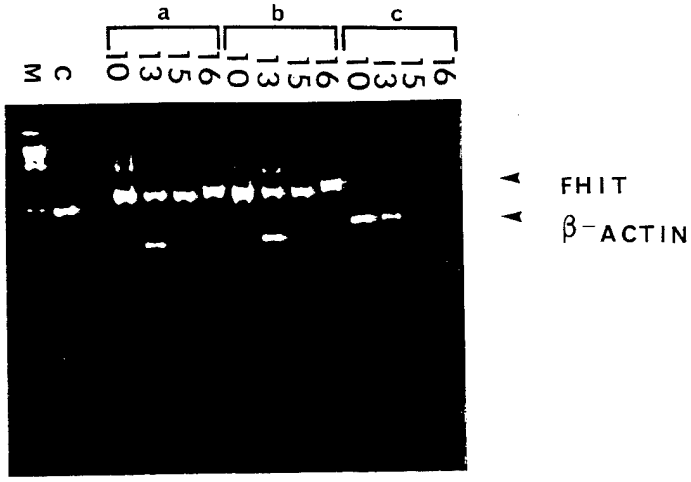
M
C
a
b
c
10
13
15
16
10
13
15
16
10
13
15
16
FHIT
β-ACTIN

Figure 1

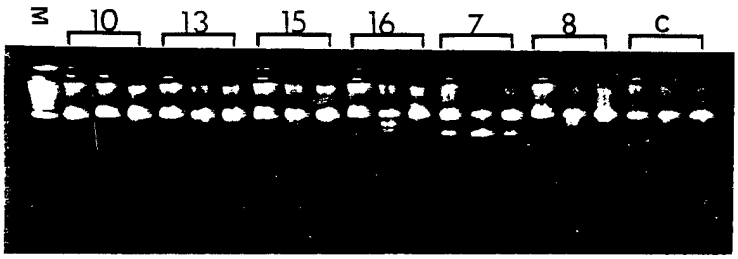

Figure 2

Table 1. Clinical and Histological data on primary breast tumors of 27 patients.

Case	Age	Diagnosis	a)TNM	Stage	Nuclear Group	Histological Group	FHIT Transcript
BC-A	47	Intraductal & Invasive Ductal Carcinoma	T2aN1Mo	II	III/III	III/III	Normal
BC-B	73	Intraductal & Invasive Carcinoma	T1NxM1	IV	III/III	III/III	Normal
BC-C	66	Intraductal & Invasive Carcinoma	T1NoMo	I	III/III	III/III	Normal
BC-D	38	Intraductal & Infiltrating Ductal Carcinoma	T1N1Mo	II	II/III	III/III	Aberrant
BC-2	56	Extensive Intraductal Carcinoma	T2NoMo	II	II/III	III/III	Aberrant
BC-3	39	Intraductal & Invasive Ductal Carcinoma	T2N1Mo	II	II/III	II/III	Aberrant
BC-6	48	Intraductal & Invasive Ductal Carcinoma	T1N1Mo	I	II/III	II/III	Normal
BC-7	39	Invasive Ductal Carcinoma	T3N1Mo	III	b)n.a.	b)n.a.	Aberrant
BC-8	41	Intraductal & Invasive Ductal Carcinoma	T2NoMo	II	II/III	II/III	Normal
BC10	53	Intraductal & Invasive Ductal Carcinoma	T3N1Mo	IV	II/III	II/III	Normal
BC13	66	Intraductal & Invasive Ductal Carcinoma	T2NoMo	II	II/III	II/III	Aberrant
BC15	39	Invasive Ductal Carcinoma	T2N1Mo	II	III/III	III/III	Normal
BC16	85	Invasive Ductal Carcinoma	T3NxMo	III	III/III	III/III	Aberrant
BC17	36	Invasive Ductal Carcinoma	T2N1Mo	II	III/III	II/III	Normal
BC18	55	Intraductal & Infiltrating Carcinoma	T1NoMo	I	II/III	II/III	Normal
BC19	62	Medullary Carcinoma	T1NoMo	I	III/III	III/III	Aberrant
BC22	59	Intraductal & Invasive Ductal Carcinoma	T1NoMo	I	III/III	III/III	Aberrant
BC23	49	Intraductal & Invasive Ductal Carcinoma	T2NoMo	II	III/III	III/III	Normal
BC24	76	Intraductal & Invasive Ductal Carcinoma	T2NxMo	II	III/III	II/III	Normal
BC25	35	Intraductal & Invasive Ductal Carcinoma	T2N1Mo	II	III/III	III/III	Normal
BC26	47	Intraductal & Infiltrating Ductal Carcinoma	T2N1Mo	II	II/III	III/III	Aberrant
BC27	31	Invasive Ductal Carcinoma	T2N1Mo	II	III/III	III/III	Normal
BC28	73	Invasive Ductal Carcinoma-Lobular Comp.	T1NxMo	I	II/III	II/III	Aberrant
BC29	79	Metastatic Adenocarcinoma	T2N2Mo	IV	III/III	III/III	Normal
BC30	59	Intraductal & Invasive Ductal Carcinoma	T2NoMo	II	II/III	II/III	Normal
BC31	33	Anaplastic Carcinoma	T4N1Mo	IV	b)n.a.	b)n.a.	Aberrant
BC32	57	Intraductal & Invasive Anaplastic Carcinoma	T4NxMo	IV	III/III	III/III	Normal

a)TNM, tumor-nodes-metastases classification
b) n.a., not available

Karyotyping human chromosomes by combinatorial multi-fluor FISH

Michael R. Speicher, Stephen Gwyn Ballard & David C. Ward

We have developed epifluorescence filter sets and computer software for the detection and discrimination of 27 different DNA probes hybridized simultaneously. For karyotype analysis, a pool of human chromosome painting probes, each labelled with a different fluor combination, was hybridized to metaphase chromosomes prepared from normal cells, clinical specimens, and neoplastic cell lines. Both simple and complex chromosomal rearrangements could be detected rapidly and unequivocally; many of the more complex chromosomal abnormalities could not be delineated by conventional cytogenetic banding techniques. Our data suggest that multiplex-fluorescence *in situ* hybridization (M-FISH) could have wide clinical utility and complement standard cytogenetics, particularly for the characterization of complex karyotypes.

Chromosome karyotyping by conventional cytogenetic banding methods is both time consuming, expensive, and difficult to automate. The detection of recurring genetic changes in solid tumour tissues by karyotyping is particularly problematic because of the difficulty in routinely preparing metaphase spreads of sufficient quality and quantity and the complex nature of many of the chromosomal changes. Marker chromosome identification based solely on banding patterns is extremely difficult. Indeed, attempts to fully automate karyotype analysis over the past twenty years have failed because robust computer algorithms could not be developed to reliably decipher complex banding patterns, particularly those of extensively rearranged chromosomes.

Fluorescence *in situ* hybridization (FISH) is a powerful tool for the analysis of genes and chromosomes because of its high absolute sensitivity and its ability to provide information at the single gene/single cell level. For this reason FISH techniques are being increasingly used in both basic research and clinical applications[1,2]. One of the advantages of fluorescence for the detection of hybridization probes is that several targets can be visualized simultaneously in the same sample. Using either combinatorial[3–5] or ratio-labelling[6–8] strategies, many more targets can be discriminated than the number of spectrally resolvable fluorophores. The simultaneous visualization of seven different probes labelled combinatorially with up to three fluors and 12 different probes labelled with different fluor ratios has been reported[5–6,9–12]. Combinatorial labelling provides the simplest way to label probes in a multiplex fashion since a probe fluor is either completely absent (0) or present in unit amounts (1); image analysis is thus more amenable to automation, and a number of experimental artifacts are avoided (such as differential photobleaching of the fluors and the effects of changing excitation source power spectrum).

The number of useful boolean combinations of N fluors is 2^N–1. Thus, for a single fluor A, there is only one useful combination (A = 1), while for two fluors, A and B, there are three useful combinations (A = 1, B = 0; A = 0, B = 1; A = 1, B = 1). There are seven combinations for three fluors, 15 combinations for four fluors, 31 combinations for five fluors, 63 combinations for six fluors, and so on. To uniquely identify all 24 chromosome types in the human genome using chromosome painting probes, five spectrally distinguishable fluors are needed. Each probe is thereby provided with a distinct spectral signature dictated by its fluor composition.

We describe a set of six fluors and corresponding optical filters spaced across the spectral interval 350–770 nm that give a high degree of discrimination between all possible fluor pairs. Using these fluors and filter sets, we have demonstrated simultaneous visualization of 27 combinatorially labelled probes applied to chromosome karyotyping by FISH, including whole chromosome paints, chromosome arm or band specific probes, and YAC clones.

Selection of fluors and high contrast filters

The limited spectral bandwidth available for fluorescence imaging (~350–800 nm), and the extensive overlap between the spectra of organic fluors, makes

Departments of Genetics and Molecular Biophysics and Biochemistry, Yale University School of Medicine, 333 Cedar St., New Haven, Connecticut 06510, USA

Correspondence should be addressed to M.R.S.

Table 1 Epicube filter configuration for 75 W Xe arc source

	DAPI	FITC	Cy3	Cy3.5	Cy5	Cy7
Excitation filter	Zeiss 365 nm	Omega 455DF70	Omega 546DF10	Ealing 35-3763	Omega 640DF20	Omega 740DF25
Dichroic beamsplitter	Zeiss 395 nm	Omega 505DRLP02	Omega 560DRLP02	Omega 590DRLP02	Omega 645DRLP02	Omega 777DRLP02
Emission filter	Zeiss >397 nm	Omega 530DF30	Ealing 35-3722	Zeiss 630/30	Omega 670DF32	Omega 780EFLP
IR blocking	Schott BG38	Schott BG38	Schott BG38	Schott BG38	Oriel 58893	Oriel 58895

separating multiple fluors spectroscopically a significant technical challenge. Choice of the fluors and filters in Table 1 was based on computer modelling of their contrast parameters using digitized excitation and emission spectra of a number of common fluors, the transmittance spectra of interference filters and dichroic beamsplitters from several optical suppliers (Omega, Ealing, Oriel and Zeiss), and the power spectra of the high pressure mercury arc, high pressure xenon arc, the Hg-Xe arc, the quartz tungsten-halogen lamp and various laser excitation sources. Excitation and emission contrast ratios were computed for every fluor relative to its two nearest spectral neighbours. Filters were then selected to achieve >90% discrimination. This level of contrast is not generally achievable using either excitation selection or emission selection alone, no matter how narrow the filter bandwidths. Thus excitation selection and emission selection were applied simultaneously. Excitation contrast was favored whenever possible, to avoid unnecessary wasting of fluorescence photons (and hence unproductive photobleaching of the fluor).

The chosen fluor set consisted of 4'-6-diamidino-2-phenylindole (DAPI, a general DNA counterstain), fluorescein (FITC), and the cyanine dyes Cy3, Cy3.5, Cy5, Cy5.5 and Cy7. The absorption and emission maxima, respectively, for these fluors are: DAPI (350nm; 456nm), FITC (490nm; 520nm), Cy3 (554nm; 568nm), Cy3.5 (581nm; 588nm), Cy5 (652nm; 672nm), Cy5.5 (682nm; 703nm) and Cy7 (755nm; 778nm). The excitation and emission spectra, extinction coefficients and quantum yield of these fluors are described[13–16]. All fluors were excited with a 75W Xenon arc.

To attain the required selectivity, filters with bandwidths in the range of 5–15 nm (compared to approximately 50 nm or more for 'standard' filter sets) were required. Further, it was necessary to both excite and detect the fluors at wavelengths far from their spectral maxima. Emission bandwidths were made as wide as possible. For low-noise detectors such as the cooled CCD camera used here, restricting the excitation bandwidth has little effect on attainable signal to noise ratios; the only drawback is increased exposure time.

Epifluorescence filter cubes constructed using the bandpass and dichroic filters listed in Table 1 were tested experimentally for spectral contrast between adjacent fluors. Good contrast (>92%) was attained in practice for all fluors except the Cy5/Cy 5.5 pair, which was marginal (80–90%). For this reason, Cy 5.5 was omitted from the combinatorial labelling experiments described below. It is vital to prevent infra-red light emitted by the arc lamp from reaching the detector; CCD chips are extremely sensitive in this region. Thus, appropriate IR blocking filters (Table 1) were inserted in the image path immediately in front of the CCD window, to minimize loss of image quality.

Imaging software

Multi-fluor combinatorial labelling depends on acquiring and analysing the spectral signature of each probe, that is, the intensity values of each of the component fluors in the six imager channels. Critical features are accurate alignment of source images, correction of chromatic crosstalk, and quantitation of the intensity of each fluor. To circumvent manual image manipulation we developed the necessary software to achieve these functions (see Methods). This software carries out the following steps in sequential order: 1) correction of the geometric image displacements caused by wedging in the emission interference filters, and by mechanical noise; 2) calculation of a DAPI segmentation mask to delineate all of the chromosomes in a metaphase spread; 3) calculation and subtraction of the background intensity values for each fluor, calculation of a threshold value, and creation of a segmentation mask for each fluor; 4) utilization of the segmentation mask of each fluor to establish a 'boolean' spectral signature of each probe; 5) visualization of the material hybridizing to each chromosome probe next to the DAPI image to facilitate chromosome identification; 6) creation of a com-

Table 2 Combinatorial labelling scheme used for the simultaneous labelling of all 24 chromosomes

a, 24-colour experiment with microdissected whole chromosome painting probes

	1	2	3	4	5	6	7	8	9	10	11	12	13	14	15	16	17	18	19	20	21	22	X	Y
Fluoroscein	x					x	x		x				x		x		x			x	x	x		x
Cy3			x		x		x		x			x	x			x			x				x	x
Cy3.5				x		x	x				x	x		x	x			x	x		x		x	
Cy5								x	x	x	x			x		x			x	x	x	x		
Cy7		x			x			x				x	x	x	x		x	x		x		x		

b, 27-colour experiment with microdissected whole chromosome painting probes and chromosome arm painting probes

	1	2	3p	3q	4	5p	5q	6	7	8	9	10	11p	11q	12	13	14	15	16	17	18	19	20	21	22	X	Y
Fluoroscein	x							x	x		x		x			x		x		x			x	x	x		x
Cy3			x	x		x	x		x		x				x	x			x			x				x	x
Cy3.5					x	x		x	x				x	x	x		x	x			x	x		x		x	
Cy5			x			x				x	x	x	x	x			x		x			x	x	x	x		
Cy7		x	x			x	x			x			x		x	x	x	x		x	x		x				

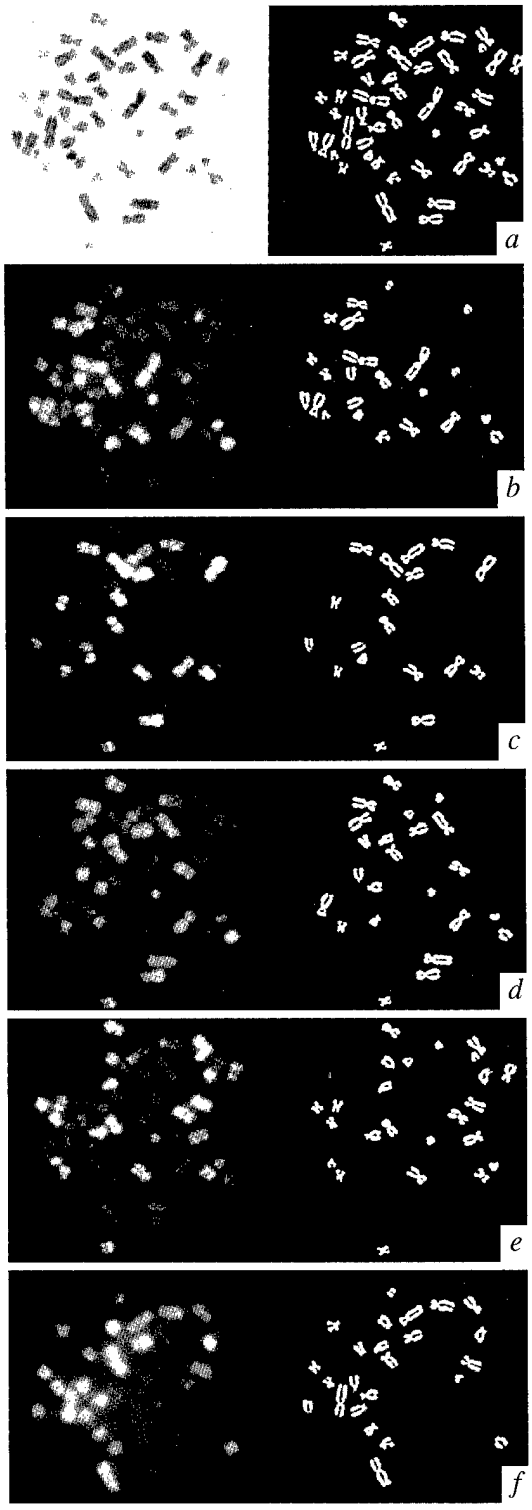

Fig. 1 Normal male metaphase spread after hybridization with a 27 DNA-probe cocktail. The left column of the figure shows the unprocessed fluorescence source images and the right column the segmentation masks computed for each fluor. *a*, DAPI: the DAPI source image was inverted to produce a G-band like pattern. *b*, FITC. *c*, Cy3. *d*, Cy3.5. *e*, Cy5. *f*, Cy7.

posite gray value image, where the material from each chromosome is encoded with a gray value; and 7) final presentation of the hybridization results using a look-up table (LUT) that assigns a pseudocolour to each such gray value.

Colour karyotyping of human chromosomes

To test the feasibility of karyotyping chromosomes by multiplex-FISH (M-FISH), chromosome painting probes representing the 22 autosomes and two sex chromosomes were combinatorially labelled, mixed, and cohybridized to normal metaphase spreads prepared from peripheral blood lymphocytes. In the case of chromosomes 3, 5 and 11 separate p and q arm probes were used; thus a total of 27 different fluor combinations were tested in this experiment (Table 2). The DNA probes were generated by microdissection and subsequent PCR amplification and labelled by nick translation (see Methods). As expected, probes labelled with equal amounts of different fluors did not give equal signal intensities for each fluor, reflecting the fact that the filter sets were selected to maximize spectral resolution rather than throughput. To diminish signal intensity differentials, probe concentrations for the hybridization mix had to be established carefully in a large number of control experiments. (For the optimized hybridization conditions, see Methods.)

A combinatorial labelling scheme was established to simutaneously label all of the 22 autosomes and the sex chromosomes (Table 2). After hybridization with the 27 probe cocktail, the fluorescence source images for DAPI, FITC, Cy3, Cy3.5, Cy5 and Cy7 were collected and the segmentation masks computed for each fluor (Fig. 1). After subtracting the interchromosomal fluorescence background from the chromosomal fluorescence, the mean of the intrachromosomal fluorescence intensities was used to calculate the threshold for creating the individual segmentation mask of each fluor (Fig. 2). Discrimination of hybridization positive and hybridization negative chromosomes was not problematic and was accomplished within a second or two.

The combinatorial labelling scheme generated a spectral signature for each chromosome (Table 2). Each of the fluor segmentation masks was interrogated by the computer program in order to establish the fluor composition of all chromosomes. For example, chromosome 7 material is labelled with FITC, Cy3 and Cy3.5 while chromosome 9 material is labelled with FITC, Cy3 and Cy5. Each of the individual chromosomes (or chromosomal segments) identified in the fluor masks on the basis of their fluor composition (its boolean spectral signature) is displayed on the computer monitor next to the DAPI image of the metaphase spread. This provides a simple means for the operator to confirm chromosome identity and to assess any chromosomal abnormalities seen in the final gray value or pseudocoloured composite images.

The karyotype of a normal male was examined using this technique. Multiple chromosome spreads (20) were analysed; the spectral signature for each chromosome was computed (Fig. 3*a*). The p and q arms of chromosome 3, 5 and 11 were labelled differentially, reflecting the use of the arm specific probes. A normal karyotype was attained as expected (Fig. 3*b*). The high efficiency of the chromosome painting achieved and the reproducibility of these results through many additional experiments using either 24

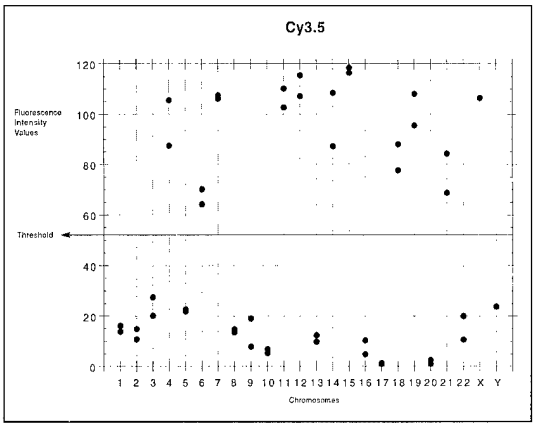

Fig. 2 Plot of the relative fluorescence intensity values for the fluor Cy3.5. Each pair of dots represents the mean fluorescence intensity values of the respective chromosome homologues. All chromosomes showing fluroescence above the threshold are represented in the Cy 3.5 mask. Note that chromosomes that were labelled with fluors very close to Cy3.5 in the spectrum, Cy3 or Cy5, but not with Cy3.5 do not have significantly increased intensity values. For example, chromosome 16 was labelled with Cy3 and Cy5 only. The intensity values over these chromosomes were no higher than any other chromosome not labelled with Cy3.5. This demonstrates the specificity of the filter used, thus allowing the unequivocal discrimination of hybridization positive and negative chromosomes.

or 27 colour labelling protocols indicated that karyotype analysis by M-FISH was feasible.

M-FISH analysis of chromosomal abnormalities

To further test the utility of M-FISH for karyotype analysis, we examined a set of five patient samples in which various chromosomal alterations had been detected by conventional cytogenetic banding techniques. These samples were provided by the Yale University Clinical Cytogenetics Laboratory and were analysed in a blind fashion using a pool of 24 whole chromosome painting probes. The karyotypes were determined by M-FISH for each of the five patient specimens (Fig. 4). The chromosomal abnormalities observed were as follows: BM2486, a chromosome 5;8 translocation (Fig. 4*a*); 10608, a 2;14 translocation (Fig. 4*b*); BM2645, a 2;3 translocation plus a deletion in 6q (Fig. 4*c*); BM2527, a 15;17 translocation (Fig. 4*d*), and BM3149, a 3;5 and a 6;12 translocation, loss of one copy of chromosomes 5 and 12 and trisomy of chromosome 8 (Fig. 4*e*). In each case, the chromosomal alterations seen by M-FISH were identical to those identified by cytogenetic banding. Furthermore, using the G-banding pattern generated by the DAPI fluorescence and measuring the fractional chromosome length of the translocation chromosomes, it was possible to infer the cytogenetic band implicated in the translocation breakpoints using fractional chromosome length/cytogenetic band conversion charts[17,18], which again agreed with the cytogenetic data. It should be noted, however, that differential chromosome condensation could lead to discordance between fractional length measurements and cytogenetic band assignments.

In some instances where the chromosomes are highly condensed there is an additional colour generated at the site of the translocation breakpoints (Fig. 4*a, c, d*). This is due to the blending of colours by fluorescence flaring at the junctions of the individual chromosome painting probe domains. This colour blending is not observed when more extended, prometaphase chromosomes, are examined (Fig. 4*b*), or when the fluor composition of both translocation chromosomes have only a single fluor difference (for example, Fig. 4*d*), where chromosome 15 was labelled with FITC, Cy3.5 and Cy7, and chromosome 17 was labelled with FITC and Cy7 only. However,

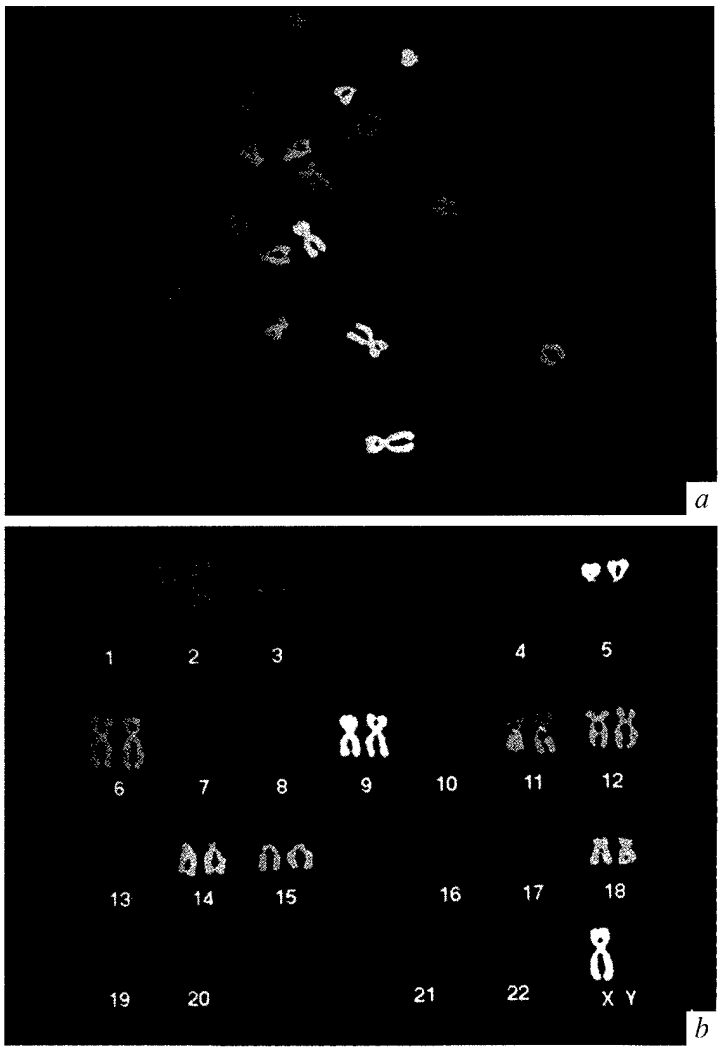

Fig. 3 *a*, Metaphase spread of Fig. 1 as a pseudocoloured image. For chromosomes 3, 5 and 11, the p and q arms were labelled differently. *b*, Final karyotype generated on the basis of the boolean spectral signature.

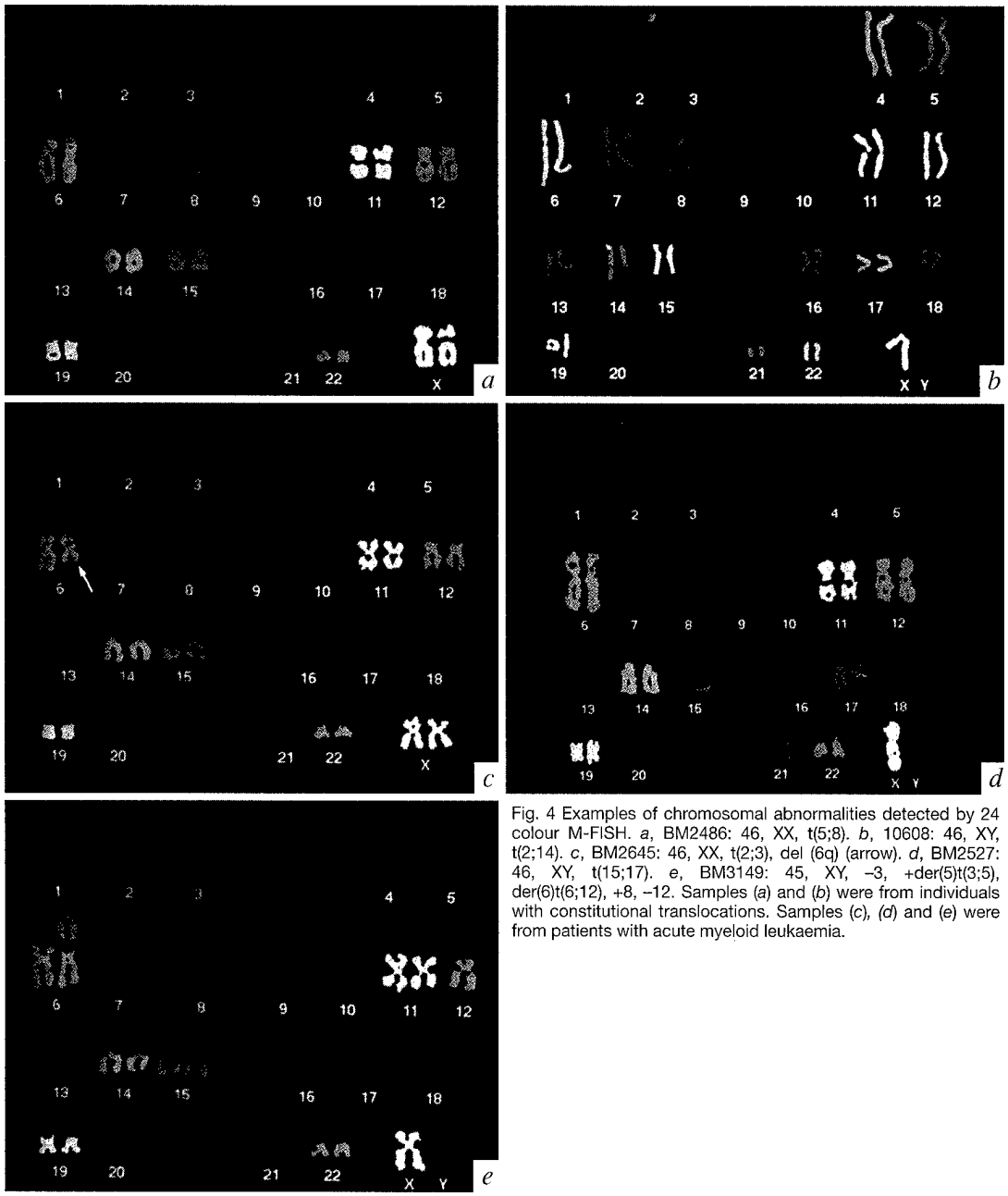

Fig. 4 Examples of chromosomal abnormalities detected by 24 colour M-FISH. *a*, BM2486: 46, XX, t(5;8). *b*, 10608: 46, XY, t(2;14). *c*, BM2645: 46, XX, t(2;3), del (6q) (arrow). *d*, BM2527: 46, XY, t(15;17). *e*, BM3149: 45, XY, –3, +der(5)t(3;5), der(6)t(6;12), +8, –12. Samples (*a*) and (*b*) were from individuals with constitutional translocations. Samples (*c*), (*d*) and (*e*) were from patients with acute myeloid leukaemia.

due to the fluorescence flaring of the Cy3.5 of chromosome 15 (Fig. 4*d*) the translocated chromosomal material from 17q appears smaller than would be expected for the recurring t(15;17)(q22;q11.2–12) in acute promyelocytic leukaemia (AML-M3). Colour blending also occurs at sites where two different chromosomes overlap in the spread. However, by examining several spreads potential problems in chromosome characterization can be avoided.

Previous studies have shown that G or R banding profiles can be generated by hybridization with oligonucleotides complementary to LINE or SINE (Alu) sequences[19,20]. Although such banding probes were not used in these experiments, it is clearly feasible to do so. However, since it is preferable to use a fluor that does not contribute to the spectral signature of the chromosomal DNAs to label the banding probe, we chose not to include hybridization banding in our protocol until we could refine the spectral resolution between Cy5 and Cy5.5. This would provide the additional fluor, Cy5.5, needed for such experiments.

We also examined several cell lines derived from patients with squamous cell carcinoma of the head and neck. These cell lines possess extensive chromosomal rearrangements and many of their chromosomes were designated only as 'marker' chromosomes when analysed by a board certified cytotechnologist using conventional cytogenetic banding procedures. One of these cell lines, HTB43, contains multiple clones with chromosome number varying between 48 and 62; many of these chromosomes are so extensively rearranged that conventional karyotype analysis is extremely difficult. Thus, finding cells that would give equivalent karyotypes by both cytogenetic banding and M-FISH is extremely difficult. In spite of this caveat, we demonstrated that M-FISH can identify complex chromosomal rearrangements not read-

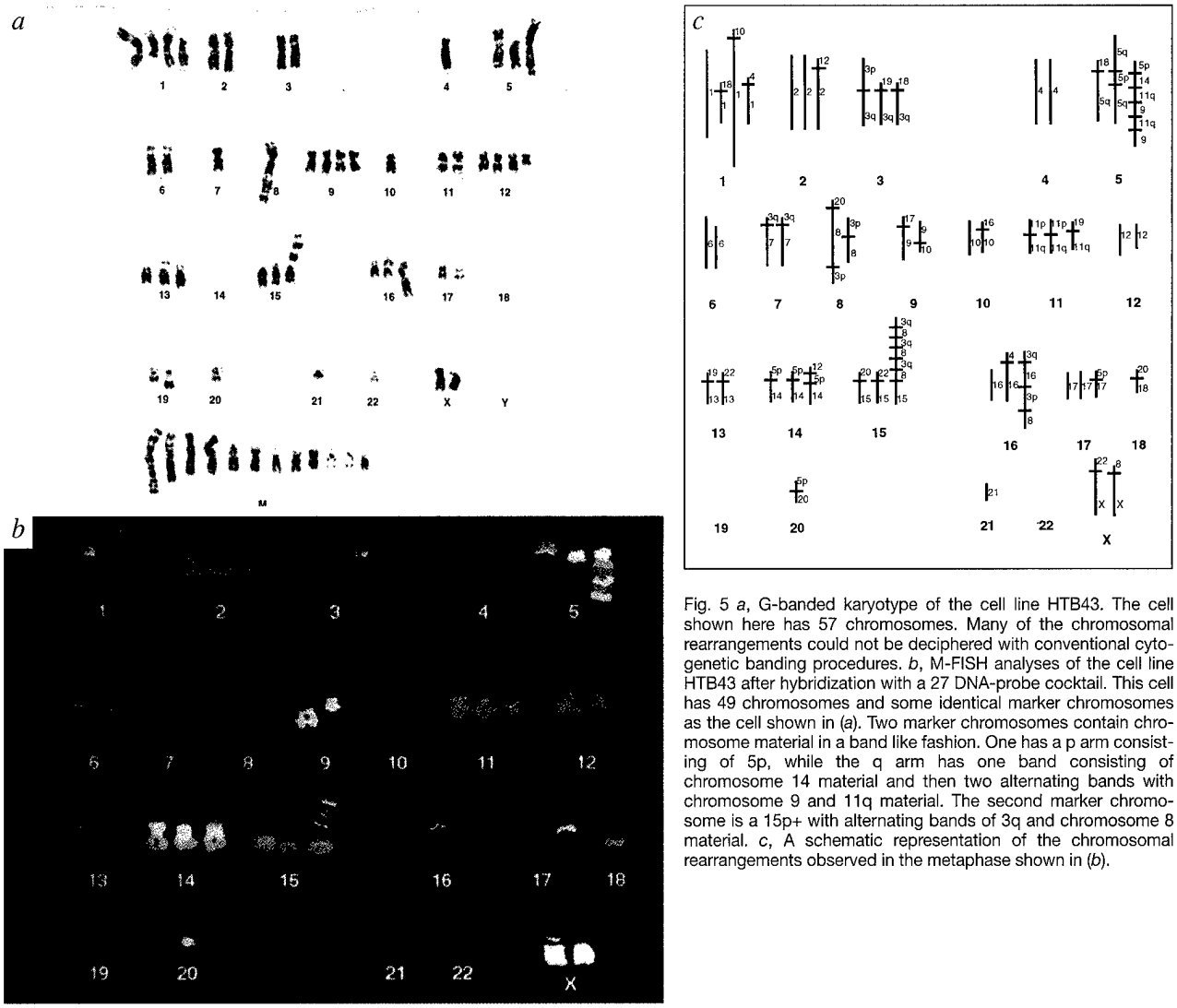

Fig. 5 *a*, G-banded karyotype of the cell line HTB43. The cell shown here has 57 chromosomes. Many of the chromosomal rearrangements could not be deciphered with conventional cytogenetic banding procedures. *b*, M-FISH analyses of the cell line HTB43 after hybridization with a 27 DNA-probe cocktail. This cell has 49 chromosomes and some identical marker chromosomes as the cell shown in (*a*). Two marker chromosomes contain chromosome material in a band like fashion. One has a p arm consisting of 5p, while the q arm has one band consisting of chromosome 14 material and then two alternating bands with chromosome 9 and 11q material. The second marker chromosome is a 15p+ with alternating bands of 3q and chromosome 8 material. *c*, A schematic representation of the chromosomal rearrangements observed in the metaphase shown in (*b*).

ily identified by conventional cytogenetic techniques (Fig. 5). M-FISH karyotype of an HTB43 cell with 49 chromosomes identified the chromosomal partners in numerous chromosomal translocations; some of the chromosomal rearrangements are extremely complex (Fig. 5*b, c*).

M-FISH with band probes and YAC clones

To determine if M-FISH could be done efficiently using regionally localized and genetically less complex probe mixtures, a set of three band specific probes from chromosome 6 were used with 19 non-chimaeric YAC clones and two whole chromosome painting probes (for chromosomes X and 8). We demonstrated that both band specific clone pools and individual YAC clones with inserts as small as 0.5 kb can be imaged and their spectral signatures correctly identified by our computer algorithms (data not shown). While the ultimate sensitivity of M-FISH has yet to be established, it should be possible to assemble probe panels to address a broad spectrum of specific biological and clinical questions.

Discussion

We demonstrate here the feasibility of discriminating up to 27 DNA probes hybridized simultaneously to metaphase chromosomes and document the ability to do karyotype analysis by multicolour FISH. Simple and complex translocations, interstitial deletions and insertions, chromosomal aneusomies and double minute chromosomes could be identified on a global basis quite rapidly. Furthermore, we were able to identify numerous chromosomal rearrangements that could not be classified by standard cytogenetic studies. Typically 5–10 metaphase spreads per case were analysed.

Defining the optimum fluor composition for each of the chromosome painting probes was done empirically through multiple hybridization experiments. Once the probe composition parameters were established, there was very little variation from one batch of probe to the next, thus highly reproducible results were obtained. These observations suggest that karyotyping by hybridization could be established in most laboratories skilled in FISH-techniques. The current software takes about 10 minutes to analyse one metaphase spread, however further refinements should reduce the analytical time significantly. Importantly, the M-FISH method is also amenable to full automation.

While we were readily able to visualize band specific probes derived from chromosome 6 and individual YAC clones containing DNA inserts of 0.5–1.0 Mb, we

have not yet tested systematically, the resolution limits of the chromosome painting probes to detect abnormalities that are routinely problematic for cytogeneticists, such as small telomeric translocations, interstitial deletions or duplications. Such studies are in progress. Since whole chromosome painting probes used in the absence of chromosome banding will not detect certain chromosomal abnormalities, for example, pericentric inversions, it is important to combine painting and banding techniques to maximize the cytogenetic information obtainable. Although pericentric inversions could be revealed if appropriate arm specific probes were used, direct banding would be preferable. Increasing the spectral resolution between Cy5 and Cy5.5, a goal that should be obtainable in the near future, would provide the additional fluor needed for banding by hybridization. The utility of M-FISH also could be extended by designing specific probe sets that stain particular chromosomal regions; telomere proximal probes for the detection of cryptic translocations, or band probes spanning translocation breakpoints associated with discrete subsets of leukemias or lymphomas. Recent advances in constructing physical and genetic maps of the human genome[21,22] and chromosome microdissection[23–27] should greatly facilitate the selection of clones to construct probe sets for specific diagnostic applications. While additional experimental evaluation will be required to define the practical advantages and technical limitations of M-FISH fully, it appears to be a versatile technique that should complement existing cytogenetic methods, particularly in characterizing complex karyotypes.

The application of M-FISH to interphase cytogenetics has yet to be explored in detail. While preliminary experiments have demonstrated the feasibility of delineating the signals from 20 chromosome-specific alphoid DNA repeat sequences by optical sectioning of cultured cells (data not shown), additional experiments will be required to determine if M-FISH can be used effectively to enumerate chromosomes in intact cells or tissues. However, with appropriate 3-D laser scanning imaging systems or algorithms for deconvoluting optical section images recorded by CCD cameras, it should be possible to analyse the intranuclear organization of whole chromosomes, defined chromosomal domains or multigene families as a function of developmental status, cell cycle stage or disease state. Such studies could provide important new insights into the architectural organization and dynamics of chromosome structure as a function of nuclear metabolic activity.

The potential utility of M-FISH is not limited to cytogenetic areas. For example, chromosomal painting probes from human or other species could be used to readily determine the location and extent of synteny between different species, thus enhancing our understanding of chromosome evolution. M-FISH could also be used to assess the presence or absence of infectious agents, define microbial serotypes or simultaneously determine not only the identity of an infectious agent but also its susceptibility or resistance to antibiotics or drugs. Multiplex gene mapping and the ability to quantitatively assess the levels of multiple mRNAs or proteins in a single cell or to determine if they exhibit different intracellular distributions could be applied to a myriad of interesting biological questions. Multiparametric imaging not only increases information throughput, it makes more efficient use of biological materials and can reveal spatial and temporal correlations, as well as mosaicisms, that otherwise might be difficult to establish reliably.

It has been suggested that the next generation of cytogenetic techniques would be molecularly based and employ multiple hybridization probes, each discriminated by a unique colour code[3,4,7,10,28]. Our studies provide a first step toward achieving this objective.

Methods

Software for analysis of combinatorially labelled probes. The program was developed using an image analysis package (BDS-Image/Oncor-Image) implemented on a Macintosh Quadra 900. Image shifts caused by optical and mechanical imperfections were corrected by alignment of the center of mass of one chromosome in each image according to a procedure described[29] and modified[30]. The DAPI image was used to define the morphological boundary of each chromosome. Chromosome segmentation was assisted by pre-filtering of each image through a top-hat filter[30,31], with the mode of the gray level histogram of the filtered DAPI image used as the threshold. For each fluor optical background was eliminated by subtracting the interchromosomal fluorescence intensity from the chromosomal fluorescence. The mean of the intrachromosomal fluorescence intensities was used to calculate the threshold for the individual segmentation mask of each fluor. Individual DNA targets were assigned distinct gray values depending on the boolean signature of each probe, that is, the combination of fluors used to label it. Finally, a look-up-table was used to assign each DNA target a pseudocolour depending on this gray value.

DNA probes. All microdissected probes were provided by J. Trent, P. Meltzer and M. Bittner (National Center for Human Genome Research, Bethesda, MD). These probes give a very uniform labelling of the target region. The detailed protocols for microdissection and PCR amplification are described[23–27]. For some chromosomes different DNA-probes for the p- and the q-arms were available, namely 2, 3, 4, 5, 10, 11, 16, 18, and Y. For all other chromosomes microdissected probes painting the entire chromosome were used.

Probe labelling. Fluorescein, Cy3, and Cy5 were linked to dUTP for direct labelling. Cy3.5 and Cy7 were available as avidin or anti-digoxigenin conjugates for secondary detection of biotin- or digoxigenin-labelled probes. They were synthesized using conventional N-succinamide ester coupling chemistry. For each probe one to four separate nick translation reactions were necessary, each with a single fluor-, biotin- or digoxigenin-labelled triphosphate (Table 2).

FISH. The reporters and the exact probe concentrations used for each chromosome paint were: 1-FITC: 110 ng; 2p-Dig: 60 ng; 2q-Dig: 200 ng; 3-Cy3: 150 ng; 3p-Cy5: 90 ng; 3q-Dig: 70 ng; 4p-Bio: 30 ng; 4q-Bio: 140 ng; 5p-Cy3: 80 ng; 5p-Dig: 70 ng; 5p-Bio: 80 ng; 5p-Cy5: 100 ng; 5q-Cy3: 170 ng; 5q-Dig: 110 ng; 6-FITC: 110 ng; 6-Bio: 60 ng; 7-FITC: 40 ng; 7-Cy3: 40 ng; 7-Bio: 20 ng; 8-Cy5: 110 ng; 8-Dig: 60 ng; 9-FITC: 110 ng; 9-Cy3: 140 ng; 9-Cy5: 120 ng; 10p-Cy5: 90 ng; 10q-Cy5: 120 ng; 11p-Bio: 20 ng; 11p-Cy5: 50 ng; 11p-FITC: 20 ng; 11p-Dig: 20 ng; 11q-Bio: 20 ng; 11q-Cy5: 60 ng; 12-Cy3: 70 ng; 12-Bio: 20 ng; 12-Dig: 60 ng; 13-FITC: 20 ng; 13-Cy3: 40 ng; 13-Dig: 40 ng; 14-Bio: 20 ng; 14-Cy5: 50 ng; 14-Dig: 40 ng; 15-FITC: 20 ng; 15-Bio: 20 ng; 15-Dig: 40 ng; 16p-Cy3: 70 ng; 16p-Cy5: 70 ng; 16q-Cy3: 90 ng; 16q-Cy5: 70 ng; 17-FITC: 30 ng; 17-Dig: 60 ng; 18p-Bio: 20 ng; 18p-Dig: 60 ng; 18q-Bio: 40 ng; 18q-Dig: 80 ng; 19-Cy3: 30 ng; 19-Bio: 20 ng; 19-Cy5: 60 ng; 20-FITC: 20 ng; 20-Cy5: 60 ng; 20-

Dig: 20 ng; 21q-FITC: 70 ng; 21q-Bio: 70 ng; 21q-Cy5: 90 ng; 22q-FITC: 100 ng; 22q-Cy5: 120 ng; X-Cy3: 40 ng; X-Bio: 20 ng; Yp-FITC: 10 ng; Yp-Cy3: 10 ng; Yq-FITC: 5 ng; Yq-Cy3: 5 ng. Thus, the total mass of labelled probe was 4.45 μg. Cot1 DNA (70 μg) and 20 μg salmon DNA were added for an overnight ethanol precipitation. On the next day the mixture of probes was resuspended in 10 μl of a conventional hybridization cocktail with 50% formamide, 2× SSC and 2% dextran sulfate.

Probes were denatured and hybridized for two to three nights at 37 °C to metaphase chromosome spreads. The slides were washed at 45 °C in 50% formamide/2× SSC three times followed by three washes at 60 °C in 0.1× SSC to remove excess probe. After a blocking step in 4× SSC/3% bovine serum albumin for 30 min at 37 °C the biotinylated probes were detected with avidin-Cy3.5 and the dig-labelled probes with anti-dig-Cy7. Fluorescein-dUTP, Cy3-dUTP and Cy5-dUTP did not require any immunological detection step. After final washes at 45 °C with 4× SSC/0.1% Tween-20 three times, mounting medium and a coverslip were applied, and the hybridization signals from each fluor were imaged using the filters sets listed in Table 1.

Cell lines. The cell lines derived from patients with squamous cell carcinoma were obtained from the American Type Culture Collection (ATCC).

Acknowledgements

We thank T. Yang-Feng and L. Gibson for karyotyped clinical samples for M-FISH analyses; T. Haaf for input during the initial stages of this work; and N. Mokady for propagation of YAC clones and cell lines. This work was supported by grant 93-018 from the Department of the Army. M.R.S. was a recipient of a grant from the Deutsche Forschungsgemeinschaft (Sp 460/1-1).

Received 11 January; accepted 20 February 1996.

1. Gray, J.W. *et al.* Molecular cytogenetics: diagnosis and prognostic assessment. *Curr. Opin. Biotech.* **3**, 623–631 (1992).
2. Xing, Y. & Lawrence, J.B. Molecular cytogenetics: applications of FISH to chromosomal aberrations in cancer genetics. In *The causes and consequences of chromosomal aberrations.* (ed. Kirsch, I.R.) 3–28 (CRC Press, Boca Raton, 1993).
3. Nederlof, P.M. *et al.* Three color fluorescence *in situ* hybridization for the simultaneous detection of multiple nucleic acid sequences. *Cytometry* **10**, 20–27 (1989).
4. Nederlof, P.M. *et al.* Multiple fluorescence *in situ* hybridization. *Cytometry* **11**, 126–131 (1990).
5. Ried, T., Baldini, A., Rand, T.C. & Ward, D.C. Simultaneous visualization of seven different DNA probes by *in situ* hybridization using combinatorial fluorescence and digital imaging microscopy. *Proc. Natl. Acad. Sci. USA* **89**, 1388–1392 (1992).
6. Dauwerse, J.G., Wiegant, J., Raap, A.K., Breuning, M.H. & van Ommen, G.J.B. Multiple colors by fluorescence *in situ* hybridization using ratio-labelled DNA probes create a molecular karyotype. *Hum. Mol. Genet.* **1**, 593–598 (1992).
7. Nederlof, P.M., van der Flier, S., Vrolijk, J., Tanke, H.J. & Raap, A.K. Fluorescence ratio measurements of double-labeled probes for multiple *in situ* hybridization by digital imaging microscopy. *Cytometry* **13**, 839–845 (1992).
8. du Manoir, S.*et al.* Detection of complete and partial chromosome gains and losses by comparative genomic *in situ* hybridization. *Hum. Genet.* **90**, 590–610 (1993).
9. Ried, T., Landes, G., Dackowski, W., Klinger, K. & Ward, D.C. Multicolor fluorescence *in situ* hybridization for the simultaneous detection of probe sets for chromosomes 13, 18, 21, X and Y in uncultured amniotic fluid cells. *Hum. Mol. Genet.* **1**, 307–313 (1992).
10. Lengauer, C. *et al.* Chromosomal bar codes constructed by fluorescence *in situ* hybridization with Alu-PCR products of multiple YAC clones. *Hum. Mol. Genet.* **2**, 505–512 (1993).
11. Popp, S. *et al.* A strategy for the characterization of minute chromosome rearrangements using multiple color fluorescence in situ hybridization with chromosome specific DNA libraries and YAC clones. *Hum. Genet.* **92**, 527–532 (1993).
12. Wiegant, J. *et al.* Multiple and sensitive fluorescence *in situ* hybridization with rhodamine-, fluorescein-, and coumarin-labeled DNAs. *Cytogenet. Cell Genet.* **63**, 73–76 (1993).
13. Ernst, L.A., Gupta, R.K., Mujumdar, R.B. & Waggoner, A.S. Cyanine dye labeling reagents for sulfhydryl groups. *Cytometry* **10**, 3–10 (1989).
14. Mujumdar, R.B., Ernst, L.A., Mujumbar, S.R. & Waggoner, A.S. Cyanine dye labeling reagents containing isothiocyanate groups. *Cytometry* **10**, 11–19 (1989).
15. Yu, H. *et al.* Cyanine dye dUTP analogs for enzymatic labeling of DNA probes. *Nucl. Acids Res.* **22**, 3226–3232 (1994).
16. Waggoner, A. Covalent labeling of proteins and nucleic acids with fluorophores. *Meth. Enzym.* **246**, 362–373 (1995).
17. Francke, U. Digitized and differentially shaded human chromosome ideograms for genomic applications. *Cytogenet. Cell Genet.* **65**, 205–219 (1994).
18. Bray-Ward, P. *et al.* Integration of the cytogenetic, genetic and physical maps of the human genome by FISH mapping of CEPH YAC clones. *Genomics* (in the press).
19. Baldini, A. & Ward, D.C. *In situ* hybridzation banding of human chromosomes with Alu-PCR products: a simultaneous karyotype for gene mapping studies. *Genomics* **9**, 770–774 (1991).
20. Matera, A.G. & Ward, D.C. Oligonucleotide probes for the analysis of specific repetitive DNA sequences by fluorescence *in situ* hybridization. *Hum. Mol. Genet.* **1**, 535–539 (1992).
21. Chumakov, I.M. *et al.* A YAC contig of the human genome. *Nature* **377**, 175–299 (1995).
22. Hudson, T.J. *et al.* An STS-based map of the human genome. *Science* **270**, 1945–1954 (1995).
23. Meltzer, P.S., Guan, X.Y., Burgess, A. & Trent, J. Rapid generation of region specific probes by chromosome microdissection and their application. *Nature Genet.* **1**, 24–28 (1992).
24. Guan, X.Y., Trent, J.M. & Meltzer, P.S. Generation of band-specific painting probes from a single microdissected chromosome. *Hum. Mol. Genet.* **2**, 1117–1121 (1993).
25. Guan, X.Y., Meltzer, P.S. & Trent, J.M. Rapid generation of whole chromosome painting probes (WCPs) by chromosome microdissection. *Genomics* **22**, 101–107 (1994).
26. Guan, X.Y., Meltzer, P.S., Burgess, A. & Trent, J.M. Complete coverage of chromosome 6 by chromosome microdissection: Generation of 14 band region-specific probes. *Hum. Genet.* **95**, 637–640 (1995).
27. Guan, X.Y. *et al.* Chromosome arm painting probes. *Nature Genet.* **12**, 10–11 (1996).
28. Ledbetter, D.H. The 'colorizing' of cytogenetics: is it ready for prime time? *Hum. Mol. Genet.* **5**, 297–299 (1992).
29. Waggoner, A. *et al.* Multiple spectral parameter imaging. *Meth. Cell. Biol.* **30**, 449–478 (1989).
30. du Manoir, S. *et al.* Quantitative analysis of comparative genomic hybridization. *Cytometry* **9**, 21–49 (1995).
31. Smith, T.G. Jr., Marks, W.B., Lange, G.D., Sheriff, W.H. Jr. & Neale, E.A. Edge detection in images using Marr-Hildreth filtering techniques. *J. Neurosci. Meth.* **26**, 75–81 (1988).

The coloring of cytogenetics

MICHAEL R. SPEICHER & DAVID C. WARD
Departments of Genetics and Molecular Biophysics and Biochemistry, Yale University School of Medicine, 333 Cedar Street, New Haven, Connecticut 06510, USA
Correspondence should be addressed to M.R.S.

Two recent papers, one from a group from Yale[1] and the other from the NIH[2] have documented the ability to identify each of the two dozen different human chromosomes — 22 autosomes and the X and Y sex chromosomes — with uniquely distinctive colors. By hybridizing sets of chromosome-specific DNA-probes, each labeled with a different combination of fluorescent dyes, to metaphase chromosome spreads it was possible to ascribe to each chromosome a unique spectral signature or identifier tag. Both approaches exploited a combinatorial probe-labeling strategy, the simplest means of generating color combinations far in excess of the number of spectrally resolvable fluorophores. As the number of useful combinations of N fluors is $2^N - 1$, only five fluorophores were needed to distinguish the 24 human chromosome types.

The Yale group[1] used a series of optical filters to image each of the five fluorophores separately and then applied a computer program to merge the separate charge-coupled device (CCD) camera images into a composite in which each chromosome was assigned a distinct color based on its fluorophore composition. In contrast, the National Institutes of Health-based consortium[2] combined Fourier spectroscopy (interferometry), CCD imaging microscopy and computer software that employed a spectral-based classification algorithm to identify the spectral characteristics of each chromosome in a single image. These methods, termed multiplex fluorescence *in situ* hybridization (M-FISH)[1] and spectral karyotyping (SKY)[2], respectively, have been shown to identify readily both simple and complex chromosomal abnormalities, features that should be applicable to pre- and postnatal diagnostics and cancer cytogenetics. Although the full potential of M-FISH and SKY in addressing problems in either the basic research or clinical arenas has yet to be assessed[3], there are a myriad of avenues now to be explored and a colorful future is promised.

Reflecting on the evolution of cytogenetics it is clear that the field has advanced through a progression of "color ages." When Theodor Boveri postulated at the turn of this century that chromosome changes would be important in the phenotype of malignant cells[4], he could not prove his theory. The means to identify individual chromosomes, not to speak of minute structural changes, were not developed. But Boveri's ingenious observations were verified many years later, and today it is common knowledge that chromosomal abnormalities are a leading cause of genetic diseases and cancer. In dividing cancer cells, pieces of chromosomes trade places inappropriately and extra chromosomes persist, resulting in highly complex and atypical karyotypes. However, it took a long time before easy and reliable methods were developed to test Boveri's central ideas. When the correct chromosome number of humans was finally established in 1956 (ref. 5), chromosome analysis depended on camera lucida drawings. Because individual chromosomes could not be identified reliably, chromosome size and the position of the centromere were used to order chromosomes into groups. We consider this period as the first color age, the "black age of cytogenetics" as only monochrome representations were done; chromosomes were drawn entirely in one color, usually black.

At the beginning of the 1970s cytogenetic analysis was revolutionized by the introduction of chromosome banding techniques[6], where chemicals revealed characteristic banding patterns along the chromosome's length. This allowed the precise identification of individual chromosomes, as well as the description of abnormal chromosome morphologies, and led over the past two decades to an explosive growth in our knowledge of tumor cytogenetics and the development of chromosome-based pre- and postnatal diagnostics. These banding techniques represent the second color age, the "black-and-white age," because they usu-

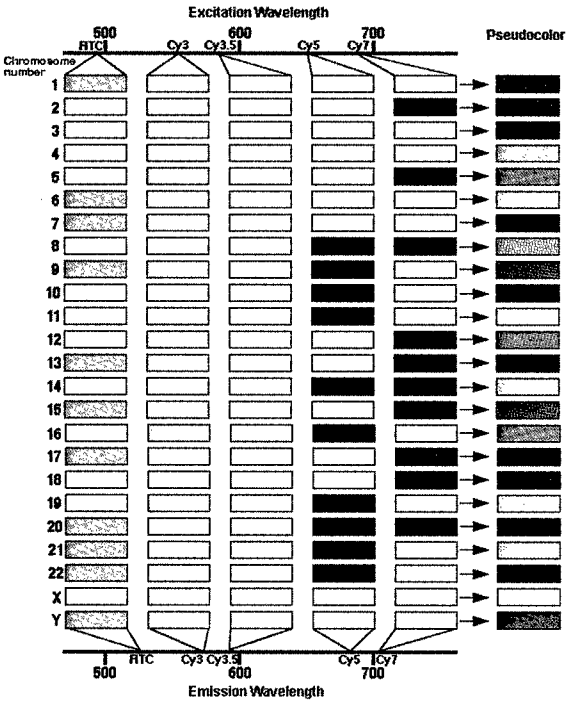

Fig. 1 Labeling scheme for a 24-color experiment. Five spectrally distinguishable fluors are needed to identify uniquely all 24 chromosome types in the human genome using chromosome painting probes. Fluors used by the Yale group are fluorescein (FITC/absorption maximum: 490 nm; emission maximum: 520 nm), Cy3 (554 nm; 568 nm), Cy3.5 (581 nm; 588 nm), Cy5 (652 nm; 672 nm) and Cy7 (755 nm; 778 nm). Each chromosome painting probe is provided with a distinct spectral signature dictated by its fluor composition. For example, chromosome 1 is labeled with FITC only, chromosome 19 is labeled with a combination of Cy3, Cy3.5 and Cy5. Each chromosome is assigned a pseudocolor, shown in the right column.

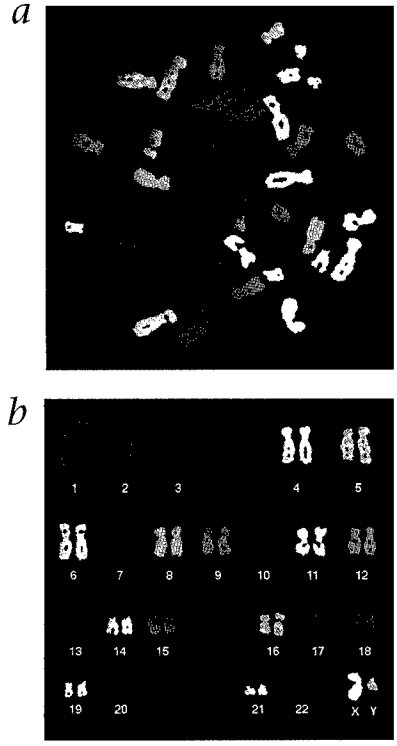

Fig. 2 *a*, Normal male metaphase spread after hybridization with a 24-DNA-probe cocktail as a pseudocolored image. *b*, Final karyotype generated on the basis of the boolean spectral signature.

ally result in alternating black and white bands. If one considers that the bands can also be illustrated in different shades of gray[7], the second color age could also be considered the "multiple gray tone" era. The contribution of banding analyses to our understanding of genetic changes in human diseases has been tremendous and pivotal for the identification of a large number of human genes. However, chromosome karyotyping by conventional cytogenetics depends critically on the quality and quantity of metaphase spreads. Complex chromosomal changes are often difficult to identify by banding methods, and little progress has been made to automate fully karyotyping based on cytogenetic bands.

"Real colors" were introduced in cytogenetics for the identification of individual chromosomes in the late 1980s and the third color age, "the FISH age" emerged. By 1988, chromosome-specific DNA probes labeled with fluors were shown to produce "chromosome paints" or to generate discrete fluorescent signals at specific loci on chromosomes[8–11]. Gene mapping by fluorescence *in situ* hybridization (FISH) became a routine research tool by 1991. Numerous cytogenetic laboratories also added FISH to their technical repertoire, using chromosome-painting probes or region-specific DNA-probes, such as yeast artificial chromosomes (YACs), for scoring chromosomal aneuploidies or translocations. However, to date, FISH has been applied largely to the detection of known chromosomal abnormalities using specific DNA probes, because for most applications some prior knowledge is necessary to select the appropriate probes.

In order for FISH to become a general screening test for chromosomal abnormalities like karyotype analysis, it was necessary to develop methods to discriminate each of the 24 distinct human chromosomes by showing each one in a different color. By exploiting the available spectrally distinct fluorophores, as well as combinatorial or ratio fluor-labeling of probes, the simultaneous visualization of three[12], seven[13–16] and even twelve[17] different probes was reported by 1993. The introduction of the cooled CCD-camera as a digital imaging device and the computer software to create pseudocolored FISH images played a pivotal role in ushering in the fourth color age, the "multicolor age." Instead of relying on real colors only, the experimenters were now free to use any color they liked. Additional fluorophores developed during the early 1990s provided novel labeling reagents and propelled the number of spectrally resolvable fluorophores beyond the five needed to distinguish all 24 chromosome types in a single hybridization experiment.

The fluors, the labeling scheme and the pseudocolors assigned to each chromosome that were selected for the experiments by the Yale group are shown in Fig. 1. As can be seen, each probe is provided with a distinct spectral signature dictated by its fluor composition. Fig. 2 shows a normal male metaphase spread after hybridization with a 24-DNA-probe cocktail as a pseudocolored image. No knowledge about chromosome morphology is required anymore, the only thing to do is to assign the colors to the right chromosome number.

The power of M-FISH to analyze highly complex tumor metaphase spreads is demonstrated in Fig. 3. Some of the rearranged chromosomes consist of fragments of up to three different chromosomes. With banding analysis alone many of these chromosome had to be assigned as "marker chromosomes." However, with M-FISH (or the SKY technique) the entire karyotype can be established in a short period of time.

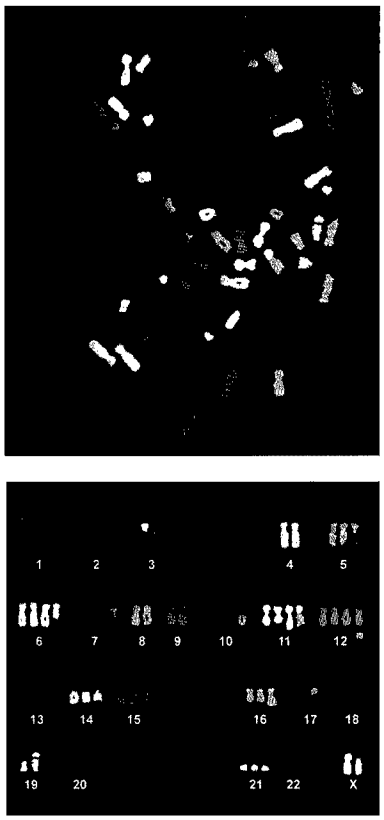

Fig. 3 Multiplex FISH allows the easy identification of highly complex tumor metaphase spreads. Many of these chromosomal rearrangements cannot be deciphered with conventional cytogenetic banding procedures. *a*, Ovarian cancer cell metaphase spread after hybridization with the same 24-DNA-probe cocktail as in Fig. 2. *b*, An accurate karyotype can easily be established on the basis of the boolean spectral signature despite the large number of rearrangements.

Future perspectives

Multiplex FISH and SKY undoubtedly will be useful for a broad range of applications from karyotyping to the elucidation of the three-dimensional (3-D) organization of the genome in intact interphase nuclei (for review see ref. 3). However, M-FISH will not, and should not, replace traditional banding analysis. We anticipate that this new technology will complement standard cytogenetics quite nicely. M-FISH using chromosome-painting probes could be used as a screening test to identify gross abnormalities. A comparison of M-FISH results with conventional cytogenetic analysis should define observed abnormalities

more precisely and should maximize cytogenetic information. For example, a comparison with cytogenetic bands should facilitate the precise identification of the exact location of breakpoints. Depending on the results, additional FISH experiments can be designed with region-specific probes either in a more conventional format or again in a multiplex fashion. Multicolor FISH with whole-chromosome painting probes does not allow the detection of intrachromosomal rearrangements; however, this problem can be overcome by multicolor bar-code strategies[14].

With respect to cancer cytogenetics, the application of M-FISH will result in the recognition of new recurring abnormalities in diseases that have been well-characterized or in tumors that have been less amenable to conventional cytogenetic studies. However, the resolution limits of M-FISH are not fully established at this point. They clearly depend in part on the probe set. For example, we do not yet know the sensitivity of M-FISH for detecting cryptic translocations. Efforts are under way to develop specific telomere-proximal probe sets for the simultaneous visualization of all telomeres in different colors. In addition, probe sets can be tailored to the needs of the respective investigator. A cytogeneticist in a prenatal laboratory will have a different focus than a colleague in a hematology laboratory. The former would be interested in a probe set that analyzes the most common numerical abnormalities and perhaps some microdeletion syndromes, whereas the latter would prefer a probe set consisting of a combination of breakpoint-spanning probes that covers all known translocations in leukemias.

In the near future even more fluors should become available for M-FISH. We have already tested the new cyanine dyes Cy2 and Cy5.5, and additional fluors, such as Cy0 and Cy1, are in preparation (A. Waggoner, personal communication). These additional fluors can be used either to decrease the labeling complexity of the existing probe sets or to add even more probes. An additional fluor should also facilitate the simultaneous use of hybridization banding with probes complementary to LINE or SINE (Alu) sequences and the automation of M-FISH with full banding capability.

Although our knowledge about the 3-D organization of the genome in intact interphase nuclei has grown significantly over the past few years (for review see ref. 18), visualizing all chromosome domains at the same time in interphase nuclei will be an intriguing challenge. The realization of such a goal, although it depends on further hardware and software development for multiplex 3-D image analysis, is clearly on the horizon.

1. Speicher, M.R., Ballard, S.G. & Ward, D.C. Karyotyping human chromosomes by combinatorial multi-fluor FISH. *Nature Genet.* **12**, 368–375 (1996).
2. Schrock, E. *et al.* Multicolor spectral karyotyping of human chromosomes. *Science* **273**, 494–497 (1996).
3. LeBeau, M.M. One FISH, two FISH, red FISH, blue FISH. *Nature Genet.* **12**, 341–344 (1996).
4. Boveri, T. in *Zur Frage der Enstehung maligner Tumoren*. 1–64 (Verlag Gustav Fischer, Jena, Germany, 1914).
5. Tjio, J.H. & Levan, A. The chromosome number of man. *Hereditas* **42**, 1–6 (1956).
6. Caspersson, T., Zech, L. & Johansson, C. Differential binding of alkylating fluorochromes in human chromosomes. *Exp. Cell Res.* **60**, 315–319 (1970).
7. Francke, U. Digitized and differentially shaded human chromosome ideograms for genomic applications. *Cytogenet. Cell Genet.* **65**, 205–219 (1994).
8. Landegent, J.E., Jansen in de Wal, N., Dirks, R.W., Baas, F. & van der Ploeg, M. Use of whole cosmid cloned genomic sequences for chromosomal localization by non-radioactive *in situ* hybridization. *Hum. Genet.* **77**, 366–370 (1987).
9. Lichter, P., Cremer, T., Borden, J., Manuelidis, L. & Ward, D.C. Delineation of individual human chromosomes in metaphase and interphase cells by *in situ* suppression hybridization using recombinant DNA libraries. *Hum. Genet.* **80**, 224–234 (1988).
10. Cremer, T., Lichter, P., Borden, J., Ward, D.C. & Manuelidis, L. Detection of chromosome aberrations in metaphase and interphase tumor cells by *in situ* hybridization using chromosome specific library probes. *Hum. Genet.* **80**, 235–246 (1988).
11. Pinkel, D. *et al.* Fluorescence *in situ* hybridization with human chromosome specific libraries: Detection of trisomy 21 and translocation of chromosome 4. *Proc. Natl. Acad. Sci. USA* **85**, 9138–9142 (1988).
12. Nederlof, P.M. *et al.* Three color fluorescence *in situ* hybridization for the simultaneous detection of multiple nucleic acid sequences. *Cytometry* **10**, 20–27 (1989).
13. Ried, T., Baldini, A., Rand, T.C. & Ward, D.C. Simultaneous visualization of seven different DNA probes by *in situ* hybridization using combinatorial fluorescence and digital imaging microscopy. *Proc. Natl. Acad. Sci. USA* **89**, 1388–1392 (1992).
14. Lengauer, C. *et al.* Chromosomal bar codes constructed by fluorescence *in situ* hybridization with Alu-PCR products of multiple YAC clones. *Hum. Mol. Genet.* **2**, 505–512 (1993).
15. Wiegant, J. *et al.* Multiple and sensitive fluorescence *in situ* hybridization with rhodamine-, fluorescein-, and coumarin-labeled DNAs. *Cytogenet. Cell Genet.* **63**, 73–76 (1993).
16. Popp, S. *et al.* A strategy for the characterization of minute chromosome rearrangements using multiple color fluorescence *in situ* hybridization with chromosome specific DNA libraries and YAC clones. *Hum. Genet.* **92**, 527–532 (1993).
17. Dauwerse, J.G., Wiegant, J., Raap, A.K., Breuning, M.H. & van Ommen, G.J.B. Multiple colors by fluorescence *in situ* hybridization using ratio-labelled DNA probes create a molecular karyotype. *Hum. Mol. Genet.* **1**, 593–598 (1992).
18. Cremer, T. *et al.* Role of chromosome territories in the functional compartmentalization of the cell nucleus. *Cold Spring Harbor Symp. Quant. Biol.* **58**, 777–792 (1993).

Bioimaging 4 (1996) 1–14. Printed in the UK

B1079505 PAP
13pp 26/11/96

Computer image analysis of combinatorial multi-fluor FISH

Michael R Speicher†, Stephen Gwyn Ballard and David C Ward

Departments of Genetics and Molecular Biophysics and Biochemistry, Yale University School of Medicine, 333 Cedar St, New Haven, Connecticut 06510, USA

Submitted 9 August 1996, accepted 2 September 1996

Abstract. Epifluorescence filter sets and computer software for the detection and discrimination of up to 27 different DNA probes using multiplex- fluorescence *in situ* hybridization (M-FISH) have been developed recently. This paper focuses on a more detailed description of the specific software developed for the analysis of M-FISH experiments. Crucial steps in the evaluation process such as standardization of image acquisition, chromosome segmentation, fluorescence background estimation, accurate measurement of fluorescence intensities and definition of thresholds will be described. The application of M-FISH and comparative genomic hybridization (CGH) for the detection of chromosomal abnormalities in squamous cell cancer of the head and neck is also reported. Finally, we try to define an acceptable 'standard' for a fully automated multicolor imaging system.

Keywords: automated computer analysis, fluorescence *in situ* hybridization (FISH), fluorescence intensity measurements, fluorescence microscopy, image analysis, image sampling, karyotyping, multicolor FISH, multiplex FISH (M-FISH)

1. Introduction

Traditionally, karyotyping has depended on the analysis of characteristic banding patterns along the length of each chromosome. However, metaphase spreads of sufficient quality and quantity are often difficult to prepare routinely. Metaphase spreads from solid tumor tissues are particularly problematic because they frequently have many chromosomal changes that are very difficult to interpret. As a consequence, robust computer algorithms for the fully automated karyotype analysis of extensively rearranged chromosomes have never been developed. In recent years, fluorescence *in situ* hybridization (FISH), using chromosome-specific DNA painting probes, has grown in popularity for the unequivocal identification of specific chromosomes or selected DNA regions within metaphase spreads. However, using only one or two painting probes per experiment characterizes only a small subset of the genome and some prior knowledge of karyotypic changes must often be available in order to select the right probes. The probability of detecting totally unexpected abnormalities increases with the number of DNA probes used at the same time. Thus, over the past few years attempts have been made to discriminate as many simultaneously hybridized probes as possible.

FISH is ideally suited for the simultaneous detection of multiple hybridisation probes because of the availability of spectrally distinct fluorophors. In addition, FISH allows the accurate quantitation of hybridization signals. The discrimination of many more targets than the number of spectrally resolvable fluorophores can be achieved using either combinatorial (Nederlof *et al* 1989, 1990, Ried *et al* 1992a, b, Lengauer *et al* 1993, Popp *et al* 1993, Wiegant *et al* 1993) or ratio-labeling (Dauwerse *et al* 1992, Nederlof *et al* 1992, du Manoir *et al* 1993) strategies.

A long awaited goal of cytogeneticists was to distinguish each human chromosome in a cell by means of specific color labeling (Ledbetter 1992). Twenty-four different colors are needed to allow the simultaneous visualization of the 22 autosomes and both sex chromosomes. Recently, we introduced epifluorescence filter sets and computer software for the detection and discrimination of up to 27 different DNA probes (Speicher *et al* 1996). This multiplex-fluorescence *in situ* hybridisation (M-FISH) allows the rapid and unequivocal detection of both simple and complex chromosomal alterations. M-FISH based on the combinatorial labeling strategy provides the simplest way to label probes in a

† To whom correspondence should be addressed. E-mail address: ward@biomed.med.yale.edu

0966-9051/96/010001+14$19.50 © 1996 IOP Publishing Ltd

multiplex fashion; each probe fluor is either completely absent (0) or present in unit amount (1). Since the number of useful Boolean combinations of N fluors is $2^N - 1$, at least five distinguishable fluors are needed for combinatorial labeling to uniquely identify all 24 chromosome types in the human genome using chromosome painting probe sets ($2^5 - 1 = 31$).

M-FISH was made feasible by recent improvements in excitation and emission filters, the development of new fluorochromes suitable for FISH, the availability of highly sensitive area imagers such as cooled charge coupled device (CCD) cameras, and increased computer performance. In the early FISH experiments, signals were subject to visual interpretation only. Visual interpretations alone are very powerful for a number of applications. However, in order to standardize FISH signals and to automate the evaluation of FISH experiments, some principles of quantitative FISH analysis, either using flow cytometry (Trask *et al* 1988, Bauman *et al* 1989) or measurements directly on metaphase spreads or interphase nuclei (Nederlof *et al* 1992) were established several years ago. More recently, image analysis in FISH was stimulated tremendously through the introduction of the comparative genomic hybridization (CGH) technique (Kallioniemi *et al* 1992, du Manoir *et al* 1993). CGH marked a new area in FISH in which many laboratories started with large scale fluorescence intensity measurements on a routine basis. Instead of manual manipulation of images, sophisticated procedures were developed for an automated evaluation with accurate assessments of fluorescence intensity values and well defined parameters for the image acquisition were established (du Manoir *et al* 1995, Piper *et al* 1995). Similarly, M-FISH depends—in addition to DNA-probe selection and hybridization quality—critically on quantitative image analysis of the fluorescence signals.

The focus of this paper will be on the image analysis part of M-FISH experiments. We describe in detail the specific software developed for analysis of the FISH signals. Crucial steps in the evaluation process such as standardization of image acquisition, chromosome segmentation, fluorescence background estimation, accurate measurement of fluorescence intensities and definition of thresholds are discussed. To validate M-FISH results a comparison with 'relative copy number karyotypes' obtained by CGH is performed. We summarize our experience so far in defining the minimal features an automated multicolor-FISH system should have.

2. Material and methods

2.1. FISH experiments

M-FISH hybridizations were carried out as described previously (Speicher *et al* 1996). All chromosome specific painting probes were provided by Drs Jeffrey Trent, Paul Meltzer and Michael Bittner from the National Center for Human Genome Research, Bethesda, MD, and were prepared from microdissected chromosomes. The detailed protocols for microdissection and PCR amplification are described elsewhere (Meltzer *et al* 1992, Guan *et al* 1993, 1994, 1995, 1996). For some chromosomes different DNA-probes for the p- and the q-arms were available, namely 2, 3, 4, 5, 10, 11, 16, 18 and Y. For all other chromosomes microdissected probes painting the entire chromosome were used.

Fluorescein, Cy3, and Cy5 were linked to dUTP for direct labeling. Cy3.5 and Cy7 were available as avidin or anti-digoxigenin conjugates for secondary detection of biotin- or digoxigenin-labeled probes. In 24-color experiments one to three separate nick translation reactions were necessary for each probe, each with a single fluor, biotin- or digoxigenin-labeled triphosphate. The combinatorial labeling scheme used for the simultaneous visualization of all 24 chromosomes in the experiments reported here was the same as that reported by Speicher *et al* (1996).

The reporters and the exact probe concentrations used for each chromosome paint are described in detail elsewhere (Speicher *et al* 1996). The mixture of probes was alcohol precipitated and resuspended in 10 μl of a conventional 50% formamide hybridization cocktail. Probes were denatured and hybridized for two to three nights at 37 °C to metaphase chromosome spreads. The slides were washed at 45 °C in 50% formamide/2×SSC three times followed by three washes at 60 °C in 0.1×SSC to remove excess probe. After a blocking step in 4×SSC/3% bovine serum albumin for 30 min at 37 °C the biotinylated probes were detected with avidin-Cy3.5 and the digoxigenin-labeled probes with anti-digoxigenin-Cy7. Probes labeled with fluorescein-dUTP, Cy3-dUTP, and Cy5-dUTP did not require any immunological detection step. After ~~final~~ washes at 45 °C with 4×SSC/0.1% Tween 20 ~~three times~~, mounting medium and a coverslip were applied and the hybridization signals from each fluor imaged using the filters sets described previously (Speicher *et al* 1996).

The CGH experiments were done as described elsewhere (Speicher *et al* 1995) and evaluated according to the standards detailed by du Manoir *et al* (1995). The cell line used (SCC15) was derived from a patient with squamous cell carcinoma and was obtained from the American Type Culture Collection.

2.2. Filter sets

The choice of fluors and filters used for M-FISH is explained in detail in Speicher *et al* (1996). In summary, the chosen fluor set consisted of 4′-6-diamidino-2-phenylindole (DAPI, a general DNA counterstain), fluorescein (FITC), and the cyanine dyes Cy3, Cy3.5, Cy5, and Cy7. The absorption and emission maxima, respectively, for these fluors are: DAPI (350 nm; 456 nm), FITC (490 nm; 520 nm), Cy3 (554 nm; 568 nm), Cy3.5

(581 nm; 588 nm), Cy5 (652 nm; 672 nm), and Cy7 (755 nm; 778 nm). The excitation and emission spectra, extinction coefficients and quantum yield of these fluors are described in detail elsewhere (Ernst *et al* 1989, Mujumbar *et al* 1989, Yu *et al* 1994, Waggoner 1995). All fluors were excited with a 75 W xenon arc. The required selectivity was attained by using filters with bandwidths in the range of 5–15 nm. The fluors had to be excited and detected at wavelengths far from their spectral maxima in order to achieve sufficient spectral discrimination. The exact epicube filter configuration, including excitation filter, dichroic beamsplitter, emission filter, and infra-red blocking filters, is given in Speicher *et al* (1996).

2.3. Image acquisition

For image acquisition a cooled charge-coupled device (CCD) camera (Photometrics, Tucson, AZ) mounted on a Zeiss Axioskop microscope was used. Images were acquired using a ×63 objective (Plan Neofluar, NA 1.25). A 75 W xenon arc lamp was adjusted to assure a homogeneous illumination of the optical field. The criteria for defining 'homogeneous illumination' were the same as published previously for CGH (du Manoir *et al* 1995). Briefly, an image of an empty field on a slide is homogeneous if the pixel intensities reach values above 0.1 using the following formula: [(maximum pixel intensity value−minimum pixel intensity value)/minimum pixel intensity]. To increase the image contrast the field diaphragm was closed to the border of the image acquisition area.

The pixel fluorescence intensity values that could be reached with our narrow bandpass filters (5–15 nm) after long exposure times were in the range of only about a tenth of the dynamic range of the CCD camera for some of the fluors (Cy3, Cy5 and Cy7). However, restriction of the excitation bandwidth had little effect on the signal to noise ratios. Thus, exposure times were chosen to reach a signal to noise ratio of at least 2.5:1. Typical exposure times were: DAPI, 8 seconds; FITC, 20 seconds; and for the cyanine dyes Cy3, Cy3.5, Cy5 and Cy7 about 40 seconds. The exposure times are relatively long compared to exposure times with standard filter sets; this is attributed to the small amount of light that comes through the narrow bandpass filters. In addition, the exposure time for the DAPI image was longer than normal because the xenon lamp intensity falls off sharply in the near-UV. Because of the small light flux coming through the narrow band filters, no detectable photo-bleaching was observed.

Images of the six fluors can be taken in any order. However, it is advisable to take the DAPI image first because it provides the most facile means to center the metaphase spread in the image. In our experiments the images were taken according to the arrangement of the fluor filters in our filter blocks, DAPI, FITC, Cy5, Cy3.5, Cy3 and Cy7, respectively. Because of imperfect chromatic correction of the objective lens in the UV, some refocusing had to be done when the filter block was shifted from DAPI to FITC. All the visible dyes appeared to be on the same focal plane as FITC, so that no additional adjustment of the focus was necessary after taking the FITC image.

Optical settings as well as the exposure time were optimized from one metaphase spread to the other. The exposure times were usually kept constant because increasing the exposure time did not result in a better signal to noise ratio. The imaging system magnification was adjusted as necessary to optimally image a single metaphase spread. For example, tumor cell metaphase spreads in the tri- or tetraploid range usually cover a larger surface area than metaphase spreads from normal cells. Accordingly, the CCD camera was adjusted when imaging tumor cell metaphases to allow the imaging of a larger field, albeit at the cost of resolution. The position of the field diaphragm was also changed appropriately, depending on the area covered by the metaphase spread.

3. Results

3.1. Program for M-FISH evaluation

The software program for M-FISH was developed using the image analysis package BDS Image (Current supplier: Oncor under the name 'Oncor Image'), and implemented on a Macintosh Quadra 900. The operator is required to select a single chromosome in each of the five fluor images and the corresponding DAPI image in order to ensure proper pixel shift correction. However, the rest of the analysis is done automatically, requiring about 10 minutes for a complete metaphase analysis. The program consists of two parts. The first part calculates the pixel shift correction and the segmentation mask for each of the fluors used (figure 1). The second part uses simple Boolean algorithms to determine the spectral signature dictated by the fluor composition.

3.2. Correction of optical shift

Pixel shift correction is necessary because of wedging in the emission filters and mechanical noise. The pixel shift correction was done according to a modification of the method reported by Waggoner *et al* (1989) that was shown to be very valuable for the pixel shift correction in CGH experiments (du Manoir *et al* 1995). Briefly, a single chromosome was selected in each of the five fluor images (FITC, Cy3, Cy3.5, Cy5, Cy7) and the DAPI image. Segmentation masks of the selected chromosome in each fluor image and the DAPI image of approximately the same area were calculated by iterating segmentation. This segmentation was used only for the correction of the optical shift. Mask gravity centroids as well as mask contours were computed. After an initial alignment, the final alignment was performed by moving the fluor image by one pixel in

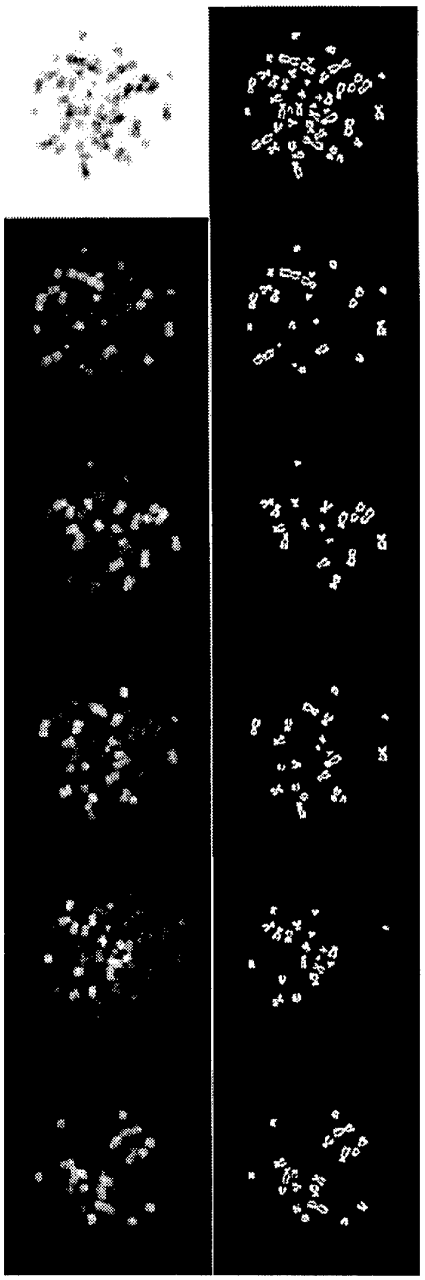

Figure 1. Normal male metaphase spread after hybridization with a 24 chromosome-specific DNA-probe cocktail. The left column of the figure shows the unprocessed fluorescence source images and the right column the segmentation masks computed for each fluor. The fluorescence banding pattern obtained after DAPI staining was used for chromosome identification. (*a*) DAPI: The DAPI source image was inverted in order to produce a G-band like pattern; (*b*) FITC; (*c*) Cy3; (*d*) Cy3.5; (*e*) Cy5; (*f*) Cy7.

the eight directions of a Freeman chain. The final position corresponds to the minimal integrated gray value in the fluor image through the border line (contour) of the chromosome mask (after binary dilatation) in the DAPI image. As a result all five fluor images are shifted to the position of the corresponding chromosome in the DAPI image.

3.3. Calculation of the DAPI segmentation mask

The first step after pixel shift correction is calculation of the DAPI segmentation mask. This was achieved after zeroing all pixel values having a gray level less than 30 out of a scale of 256. The gray level of 30 was chosen because with the selected exposure times gray levels less than 30 are significantly below gray levels from chromosomes; thus these pixels correspond to background. A 'mexican hat' convolution (13×13 pixels; Smith *et al* 1988) was then applied. The mode of the gray level histogram of the hat filtered DAPI image was used as the threshold. Holes inside the chromosome segmentation masks smaller than 300 pixels were filled. This procedure is essentially the same as that used previously for the calculation of DAPI segmentation masks for CGH-experiments (du Manoir *et al* 1995).

3.4. Calculation of the segmentation masks for FITC, Cy3, Cy3.5, Cy5 and Cy7

The calculation of the segmentation masks was done individually for each fluor using the same algorithm (figure 1). First, the background was calculated from the fluorescence intensity of the entire image. To avoid falsely elevated background values, nuclei which usually have high intensity values had to be erased manually if they covered large regions of the image. The background was subtracted from the entire image. The intrachromosomal fluorescence intensity values were then calculated and its mean value used to calculate the threshold. After applying the threshold the segmentation mask was overlayed with the DAPI segmentation mask. A simple Boolean 'AND' procedure was used to set to zero pixels that were not inside the DAPI and the respective fluor segmentation mask simultaneously. Application of the Boolean 'AND' operation allowed the accurate assignment of the borders of chromosomes in their respective fluor images. Incomplete DNA segments within a chromosome which might be caused e.g. either by a translocation or insertion event are problematic. Due to flaring of the fluors these DNA segments often appear larger than the actually painted DNA region. The threshold value and the 'AND' operation alone did not allow one to determine the borders of these painted segments within the chromosome with high accuracy. In order to improve the detection of borders of painted DNA-segments within chromosomes we took advantage of the fact that these are associated with a sharp change of fluorescence intensity values, either a sharp increase or decrease. Thus, an additional filtering in the form of a 'hat' convolution (3 × 3 pixels) was applied in order to improve the definition of

borders of painted segments within a chromosome. In addition, non-specific hybridization signals with intensity values above the threshold were also reduced drastically in size by applying the 'hat' convolution. As a final step, small fluorescent objects (< 40 pixels) were erased and small holes (< 30 pixels) in the segmentation masks were filled to increase the homogeneity of the segmentation masks.

While the calculations for all five fluors were based on the same algorithm it should be noted that these calculations were done individually for each fluor. Thus, for each metaphase spread background and threshold calculations were done six times, once for each fluor.

3.5. Presentation of results

The second part of the program utilizes the segmentation mask of each fluor to establish a Boolean spectral signature of each probe. Each of the individual chromosomes or chromosome segments identified in the fluor masks on the basis of their fluor composition is displayed on the computer monitor next to the DAPI image of the metaphase spread (figure 2). This provides a simple means to confirm chromosome identity. Finally, a composite gray value image is created, where the material from each chromosome is encoded with a gray value. A look-up table (LUT) is used to assign a pseudocolor to each such gray value (figure 3).

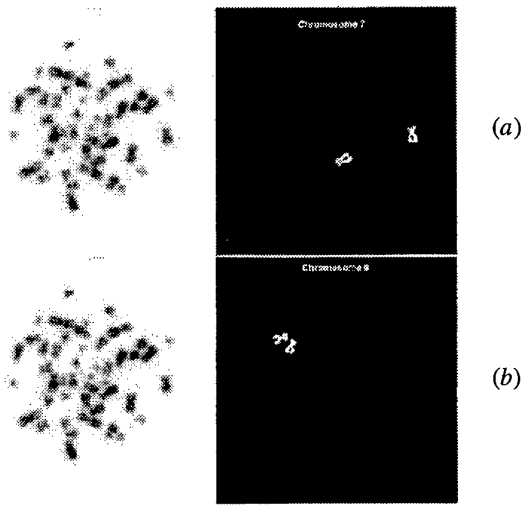

Figure 2. Individual chromosome pairs identified on the basis of their fluor composition displayed next to the DAPI image of the metaphase spread. For example, chromosome 7 is labeled with a combination of Fluoroscein (compare figure 1(*b*)), Cy3 (figure 1(*c*)) and Cy3.5 (figure 1(*d*)) but not with Cy5 (figure 1(*e*)) or Cy7 (figure 1(*f*)). Thus, a simple Boolean 'AND' operation like 'display everything that is labeled with a combination of Fluorescein AND Cy3 AND Cy3.5' will result in the identification of chromosome 7 as shown in figure 2(*a*). This part of the computer program facilitates the identification of material derived from each chromosome in the metaphase spread. Figure 2(*b*) shows the identification of chromosome 9.

3.6. Quality controls

To monitor hybridization efficiency the program prints tables with the mean fluorescence intensity of each chromosome for each fluor. These tables can easily be converted into plots of the relative fluorescence intensity values for each fluor as shown in figure 4. Each pair of dots represents the mean fluorescence intensity values of the respective chromosome homologues. In addition, the threshold value can easily be included. All chromosomes with fluorescence intensity values above the threshold are represented in the respective segmentation mask. This plot allows an easy check for (a) the signal to background ratio, (b) whether all DNA probes have the expected fluorescence intensities and (c) the discrimination of hybridization positive and negative chromosomes. Thus, these tables serve as a fast and reliable control of the quality of the M-FISH experiment.

3.7. M-FISH preparation

Probes labeled with equal amounts of different fluors did not give equal signal intensities for each fluor. This reflects the fact that the filter sets were selected to maximize spectral resolution rather than throughput. To diminish signal intensity differentials, probe concentrations for the hybridization mix had to be determined carefully in a large number of control experiments. It is critical to avoid residual cytoplasm in metaphase spreads; thus a pretreatment with RNAse and Pepsin was often necessary.

3.8. Suppression *in situ* hybridization

M-FISH depends on efficient suppression of interspersed, repetitive sequences. This is achieved by adding an excess of nonlabeled Cot1 DNA to the hybridization mixture. Usually, this results in an apparent lack of painting of tandemly repetitive DNA blocks contained in the constitutive heterochromatin of the chromosomes, for example 1q12, 9q12, 16q12, and 19cen. However, occasionally some weak staining of the heterochromatic blocks, most often at the acrocentric chromosomes of the D-group (chromosomes 13–15) was observed (see below).

3.9. Establishing parameters for M-FISH in a series of hybridizations on normal metaphase spreads

To establish the necessary parameters for M-FISH experiments, a large series of control experiments were done on metaphase spreads from healthy female and male donors. These experiments were critical to diminish signal intensity differentials between probe sets and to establish appropriate probe concentrations for the hybridization mix. Our findings were that not all labeling schemes

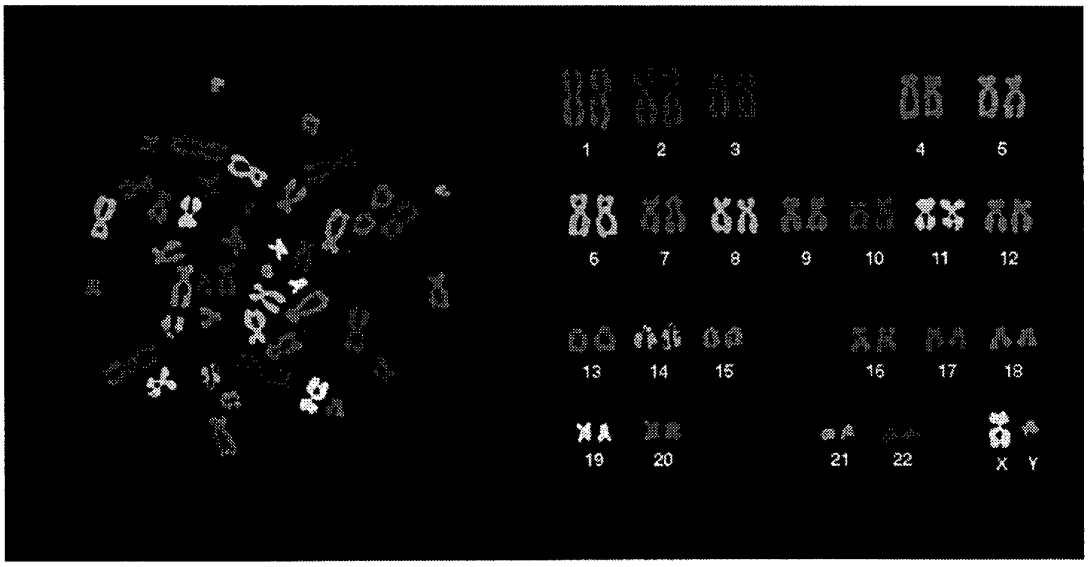

(*a*) (*b*)

Figure 3. (*a*) Metaphase spread of figure 1 as a pseudocolored image. (*b*) Final karyotype generated on the basis of the Boolean spectral signature. Note that the heterochromatic block of chromosome 14 has a different color from the q-arm due to some non-specific staining (for details see text).

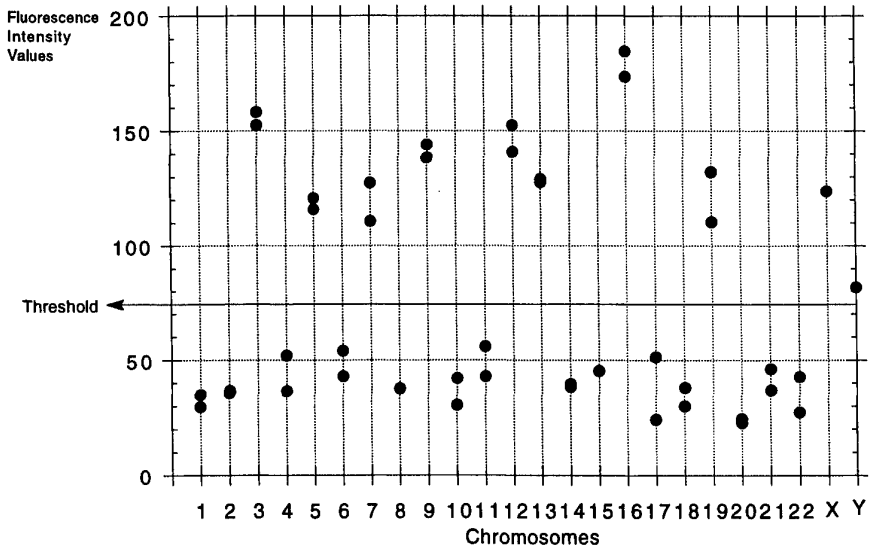

Figure 4. Plot of the relative fluorescence intensity values for the fluor Cy3. Each pair of dots represents the mean fluorescence intensity values of the respective chromosome homologs. This provides an easy mean for the operator to control the efficiency of the hybridization. In addition, it demonstrates the specificity of the filter used and the unequivocal discrimination of hybridization positive and negative chromosomes.

work with the same efficiency. Some fluor combinations yielded consistently weak hybridization signals for some chromosomes. For example, whenever the painting probe for chromosome 10 was labeled in a combinatorial fashion that included Cy3, the Cy3 signal was only weakly detectable or not observed at all. When the same probe was labeled only with Cy3 it painted chromosome 10 very well. Thus, for reasons not yet understood some combinatorial labeling schemes do not work well or in a highly reproducible fashion. The labeling scheme presented by us earlier (Speicher *et al* 1996) works very reliably; however, there may exist other labeling schemes that work equally well.

A typical example of the results of an M-FISH

experiment is shown in figure 1. This figure shows a male metaphase spread after hybridization with the 24 probe cocktail. The fluorescence source images for DAPI, FITC, Cy3, Cy3.5, Cy5 and Cy7 are shown in the left column of the figure while the segmentation masks computed for each fluor are illustrated in the right column. Note that although the experiment was done with an excess of Cot 1 DNA the heterochromatic block of chromosome 14 shows some non-specific staining with FITC. This phenomenon is observed occasionally, but usually does not interfere with the interpretation of the hybridization results.

The segmentation masks are used to identify each of the individual chromosomes on the basis of their fluor composition (i.e. its Boolean spectral signature). To provide a simple means for the operator to confirm chromosome identity and to assess any chromosomal abnormalities, individual chromosomes can be displayed on the computer monitor next to the DAPI image of the metaphase spread. Figure 2 documents the identity of two of the chromosome pairs, chromosome 7 and chromosome 9, present in the metaphase spread shown in figure 1. Chromosome identification by M-FISH was compared with that obtained by examining the fluorescence banding pattern obtained after DAPI staining. A grayscale inverted DAPI image was used because it resembles Giemsa banding.

Another feature of the M-FISH software is that the operator can easily check the distribution of the relative fluorescence intensity values for each single fluor. Figure 4 documents the signal differential between hybridization positive and hybridization negative pairs of homologous chromosomes for the fluor Cy3. All chromosomes showing fluorescence intensities above the threshold are represented in the Cy3 mask. By evaluating each of the fluor signals in this quantitative fashion, one can readily assess the specificity and signal to noise ratios obtained for each M-FISH experiment.

Figure 3(*a*) shows the metaphase spread in figure 1 as a pseudocolored image which allows the easy generation of a karyotype on the basis of the spectral signature of each chromosome as shown in figure 3(*b*). The karyotype is that expected for a normal male cell. In order to establish the prerequisite experimental parameters and to test the robustness of this technique about 20 hybridizations to chromosomes from normal female and male donors were done. After the robustness of M-FISH was verified on normal karyotypes we started with a series of blind experiments on clinical specimens with known chromosomal aberrations (Speicher *et al* 1996). These experiments confirmed that karyotype analysis by M-FISH was indeed feasible and documented a complete concordance between the results obtained by M-FISH and conventional cytogenetics. We have subsequently analysed highly complex cell lines that are not readily analysable by normal karyotyping and have used M-FISH to further define chromosomal abnormalities detected by CGH (see below).

3.10. Analysis of extensively rearranged chromosomes by M-FISH and CGH

A detailed analysis was done with the cell line SCC15 obtained from a squamous cell cancer of the head and neck region. This cell line has a large number of different clones that are so extensively rearranged that a characterization by standard banding methods is virtually impossible. In order to compare the M-FISH results with an established method, we generated a 'relative copy number karyotype' by CGH as shown in figure 5. Two exemplary M-FISH karyotypes are shown in figures 6(*b*) and 6(*e*). Previous CGH results from squamous cell cancers of the head and neck region had shown that overrepresentations of 3q and 5p and underrepresentations of 3p and 5q are nonrandom and the most frequently occurring numerical changes in this tumor (Speicher *et al* 1995). In addition, some tumors demonstrate an overrepresentation of the 11q13 region as well as an overrepresentation of 8q. The CGH ratio profile in figure 5 represents the summary of all clones, thus, the M-FISH data from a single metaphase spread of this multiclonal cell line should not necessarily correlate exactly with the 'relative copy number karyotype'. Since the use of whole chromosome painting probes does not provide information about subregions of any particular chromosome it is difficult or even impossible to estimate how many regions should be painted by a total chromosome 8 painting probe even though 8q appears to be overrepresented by CGH. In order to facilitate the comparison between M-FISH and the CGH-data we decided on a 27 color experiment using separate p and q arm probes for chromosomes 3, 5 and 11. In the metaphase shown in figures 6(*a*) and (*b*), two copies of 3p were identified while there were 4 copies of 3q. An inverse pattern was found for chromosome 5; only one copy of 5q was found but 4 copies of 5p. Thus, even with the acknowledged limitations, there was an excellent agreement between the CGH and M-FISH data.

One striking observation was that individual metaphase spreads from the SCC15 cell line differed from each other to a large extent. For example, the metaphase in figures 6(*a*) and (*b*) has a large number of rearranged chromosomes 9 while the metaphase in figures 6(*d*) and (*e*) has a large number of rearranged chromosomes 8. Some changes were consistently observed in all metaphase spreads, e.g. translocations between chromosomes 1 and 19, 22 and 3q, 5p and 13, 21 and Y. Many, but not all, metaphase spreads demonstrated a small number (1–4) of double minute chromosomes (DMs). These DMs were identified as chromosome 1 material. Thus, M-FISH should also be useful to identify DMs.

The large number of rearrangements present in many tumor cells, such as the SCC15 line, makes an interpretation based only on the color code difficult. Conversion of the color code into a 'stick model' makes it much easier to visualize all of the abnormalities present in a single metaphase spread (figures 6(*c*) and (*f*)).

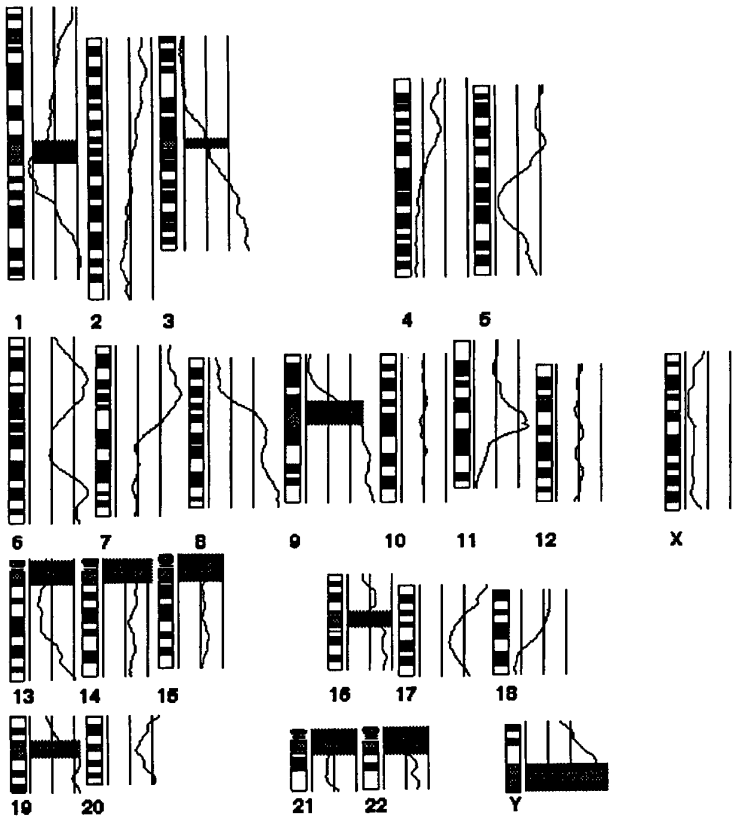

Figure 5. Average ratio profile of tumor cell line SCC15. Ratio profiles along the individual chromosomes are shown on the right side of each chromosome. Left, middle and right vertical lanes represent the lower, middle and upper threshold of the normal range. Due to the suppression with Cot1-DNA fraction the heterochromatic blocks yield unreliable ratio values and are excluded from evaluation. Relative overrepresentations were seen at 1q32-qter, 3q, 5p, 6p11-22, 6q24-qter, 7p, 8q, 9q, 11q12-14, 17p, 19q. Relative underrepresentations were observed at 3p, 4q22-qter, 5q21-23, 8p12-pter, 9p21-pter, and 18q21-qter.

4. Discussion

In this paper we have explained how we evaluate an M-FISH experiment and demonstrated its power by analysing chromosomes from a highly complex rearranged tumor cell line. This new technology represents a potentially powerful complement to standard cytogenetics. We further anticipate that applications in basic research, such as defining the topography of the interphase nucleus, will also benefit from M-FISH in the near future. Below we discuss some aspects of the imaging process, limitations of the method and approaches to develop a multicolor standardized imaging system.

4.1. Comparison of M-FISH imaging and CGH imaging

In CGH, exposure times are chosen for each fluorochrome to obtain maximum chromosomal pixel values that equal one-half of the dynamic range of the camera (du Manoir *et al* 1995). It is impossible to use the same criteria for M-FISH because the bandwidths of our filters are in the range of 5–15 nm compared to about 50 nm or more for standard filter sets. In addition, it is necessary in M-FISH to both excite and detect the fluors at wavelengths far from their spectral maxima. This results in significantly decreased pixel fluorescence intensity values that, even after relatively long exposure times, reach only about a tenth of the dynamic range of the CCD camera for some of the fluors (Cy3, Cy5 and Cy7). The most important criterion for M-FISH exposure time is not the dynamic range of the CCD camera but the signal to noise ratio. A signal to noise ratio of 2.5:1 is usually good enough for an accurate evaluation.

In CGH optical settings as well as the exposure time are usually kept constant for the images recorded from a series of metaphase spreads for a single specimen (e.g. tumor) (du Manoir *et al* 1995). This is not the case for M-FISH because M-FISH is the analysis of individual metaphase spreads. In contrast to CGH evaluations there is no averaging or combining of fluorescence intensity values

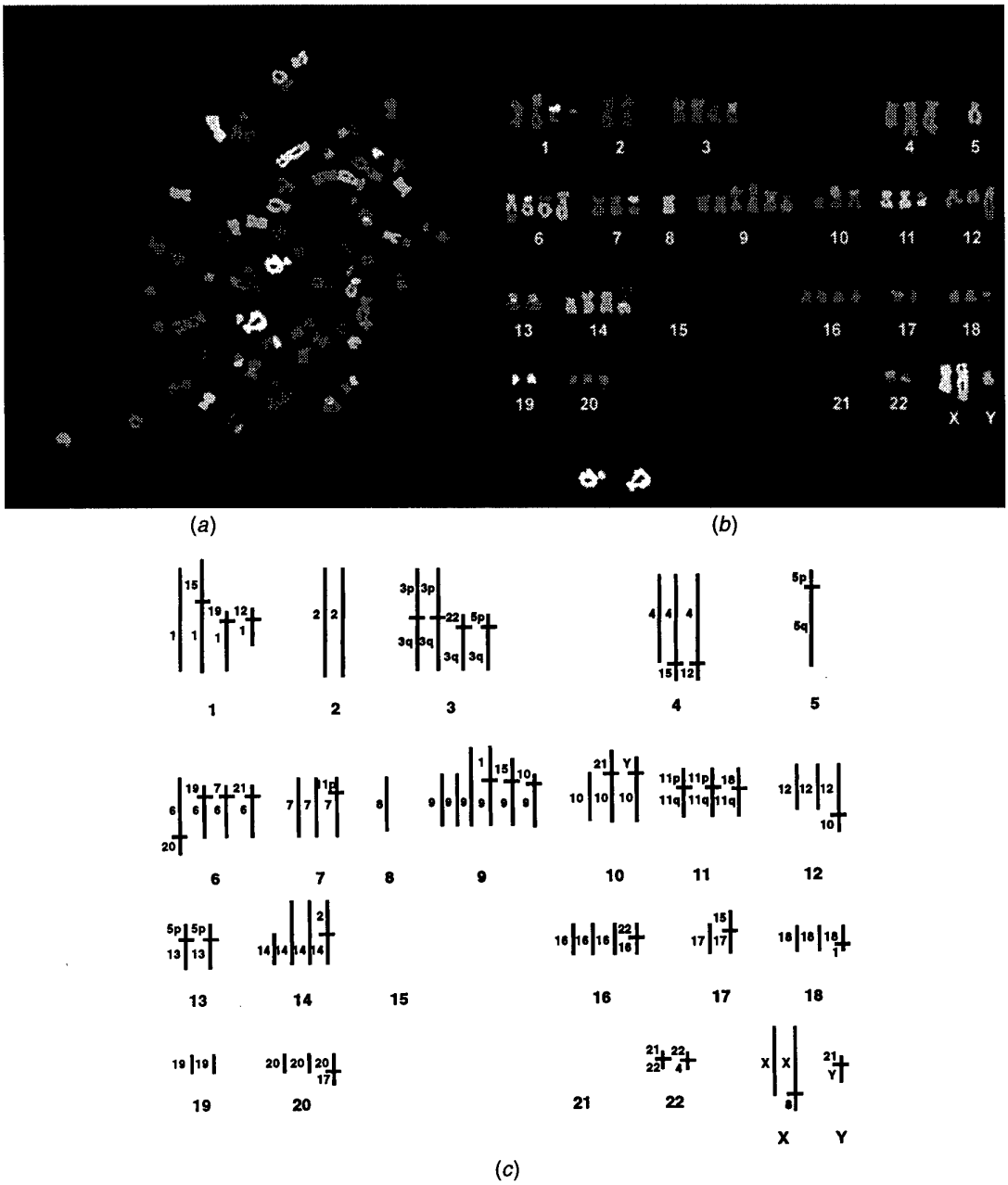

Figure 6. Two metaphase spreads (*a*)–(*c*) and (*d*)–(*f*), respectively, from cell line SCC15 after hybridization with a 27 DNA-probe cocktail. (*a*) and (*d*) show the metaphase spread, (*b*) and (*e*) the karyotypes generated on the basis of the Boolean signature, (*c*) and (*f*) 'stick models' of the karyotypes shown in (*b*) and (*e*), respectively. For chromosomes 3, 5 and 11 the p and q arms were labeled differentially. Both metaphase spreads have some chromosomes that could not be interpreted due to overlapping DNA regions, these chromosomes are displayed in white (for details see text). Note that in both metaphases there is no nullosomy of chromosome 21. Chromosome 21 material was translocated to chromosomes 6, 10, 22 and Y in the metaphase shown in (*a*) and (*b*) and to the two chromosomes Y in the metaphase shown in (*d*) and (*e*). Similarly, chromosome 15 is not completely lost in the metaphase shown in (*a*) and (*b*) but chromosome 15 segments are translocated to chromosomes 1, 4, 9 and 17. Chromosome 22 material in the metaphase in (*d*) and (*e*) is translocated to 3q and 4.

(*d*) (*e*)

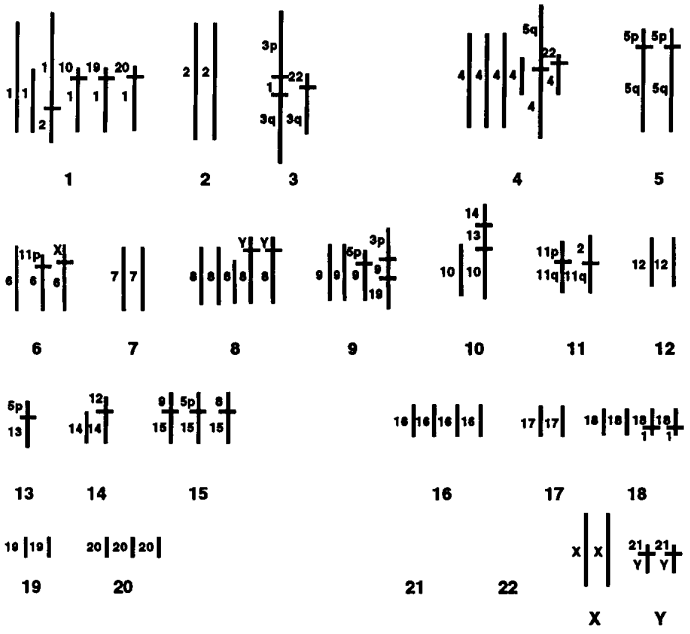

(*f*)

Figure 6. Continued.

from several metaphase spreads. Thus, optical settings can vary from one metaphase spread to the other, so that optimal imaging parameters can be achieved.

Similar to CGH, the large heterochromatic blocks [1q12, 9q12, the acrocentric chromosomes of the D-group (chromosomes 13–15), 16q12, 19cen] cannot be evaluated by M-FISH. These regions should be completely suppressed because an excess of unlabeled Cot-1 DNA is added to the hybridization mix. However, occasionally a nonspecific, but intense staining of these regions is observed. This unspecific staining is usually only observed at the acrocentric chromosomes of the D-group; staining of the heterochromatic region of chromosome 14 is the most common observed artifact (see figures 1 and 3). We do not attribute this phenomenon to the quality of the painting probes, since this additional staining occurs in less than 5 per cent of the cases analysed. It is important to note that this nonspecific staining does not interfere with the interpretation of the M-FISH results.

4.2. Regions difficult to assess with M-FISH

As with CGH, overlapping chromosomes are problematic. In such overlapping regions high fluorescence intensity values are observed that often flare into adjacent regions and interfere with the karyotypic interpretation by creating 'false spectral combinations' or 'nonexisting combinations'. For example, if chromosome 1, labeled with FITC only, overlaps with chromosome 2, labeled with Cy7 only, in the overlapping region our software would according to our look up table detect a combination of FITC and Cy7 and assign this segment to chromosome 17 which is labeled with the FITC and Cy7 combination. Should chromosome 1, labeled only with FITC, overlap with chromosome 14, labeled with Cy3.5, Cy5 and Cy7, the overlap would result in the combination FITC, Cy3.5, Cy5 and Cy7, a combination that does not exist for any chromosome. Ideally one would examine metaphase spreads without any overlaps; this is, of course virtually impossible in most clinical specimens. In particular, tumor metaphase spreads in the triploid range as shown in figure 6 almost always have some overlapping regions. Such overlapping chromosomes are depicted in white in figure 6 to indicate that M-FISH cannot delineate these regions accurately.

The resolution limits of M-FISH still have not been explored extensively. Thus, we cannot judge the performance of M-FISH to detect petite or cryptic translocations at this point. Nevertheless, it is clear that the resolution depends significantly on the selected probe set; YAC DNA clones as few as 500 kbp of human DNA can be visualized readily (Speicher *et al* 1996). Efforts are under way in our laboratory to simultaneously hybridize peritelomeric YAC- or BAC-probes to visualize all telomeric regions in different colors. Such a probe set should be an extremely powerful tool to screen for cryptic translocation events.

4.3. M-FISH compared to interferometer based spectral imaging

The simultaneous visualization of all human chromosomes in different colors has also been achieved using an approach that combines Fourier spectroscopy, CCD-imaging and optical microscopy to distinguish multiple spectrally overlapping probes (Schrock *et al* 1996). Interferometry is used to generate a discrete spectrum of fluorescence emission wavelengths detected by each pixel in a CCD chip array. A computer software program that employs a spectral-based classification algorithm then identifies the various spectral components in the image and assigns each a pseudo-color. The use of an interferometer seems to be a very attractive alternative, but a filter-based system offers several advantages.

First, the collection of separate images for each fluor offers an additional internal control of experimental results; images of each individual fluor can be inspected visually to ensure that each chromosomal segment is properly assigned. This option might be very important when smaller region-specific probes (YACs, cosmids) are used. While we have demonstrated already that M-FISH allows the simultaneous hybridization of a large number of YAC-clones, these probes are more difficult to image than chromosome-specific painting probes. This is because small region-specific probes result in signals that are often in different focal planes even on normal metaphase spreads. Thus, while signals from most YACs will be in the same focal plane several may be outside of the focal plane. This would result in some YACs with significantly reduced, or even not measurable, fluorescence intensity values. In such cases a visual evaluation of individual fluor images might be essential to rule out false positive artifacts. The development of a highly reliable imaging system for numerous 'small-probes' hybridized simultaneously, might require the scanning of metaphase spreads in multiple focal planes.

Second, the use of an individual filter set for each fluor allows an easier optimization of excitation and emission allowing the use of the entire spectrum for the selection of fluors. For example, fluors in the infrared range require different infrared blocking filters than fluors in the green range. Thus, with the filter system fluors, such as FITC and Cy7, can easily be used in the same experiment. In contrast, a system that has to excite and emit all fluors simultaneously will not be able to use FITC and Cy7 efficiently. The fact that all fluors have to be excited and emitted at the same time in the interferometer based system results in additional limitations. The wavelengths that are used for the emission cannot be used at the same time for the excitation of other fluors. This means that although the interferometer has the potential to discriminate fluors close in the spectrum, the number of usable fluors is limited to a small fraction of the spectrum. The smallest distances in terms of excitation and emission wavelengths that we could resolve with our filter system was between Cy3 and Cy3.5 and was 27 nm and 20 nm, respectively. This demonstrates that the filter system also has the capability of discriminating fluors that are close together in the spectrum. With the potential of having the entire spectrum available, we anticipate that additional fluors can be added more easily to the filter system.

Third, data obtained with a filter system are easier to interpret. A direct representation of results can easily be achieved, either in a multicolor or in a black and white fashion, e.g. the visualization of individual chromosome material (figure 2). In contrast, images obtained with the interferometer currently yield color representations of the chromosomes only. Similar colors are difficult to discriminate and depend on time consuming measurements of spectra. It is arguable that interferometry (or any other high-resolution spectral analysis method) provides far more information than needed. The full spectrum of each combinatorially labeled object pixel is not required for identification: only a spectral signature is required. The

easiest way to generate such a signature is by analysis of the relative fluorescence intensities in a small number of well separated spectral channels.

The disadvantage of the filter-based system of having to take several images can easily be overcome because the entire imaging process is amenable to automatization. Instead of moving filter blocks manually we anticipate that in the near future automated filter wheels will be available. After selecting a metaphase spread in the DAPI image the operator will have to press only one button and images from the different fluors can be taken in a completely automated fashion under conditions where possible pixel shifts can be minimized by appropriate filter alignment and computer software.

4.4. Built-in quality controls and correct presentation of result as standard for automated multicolor imaging system

The multi-fluor FISH area is just at its beginning. In our opinion some features, e.g. built in quality controls and the ability to evaluate the representations of individual chromosome results, have already emerged as important components in developing an acceptable standard for a fully automated multicolor imaging system. These and other prerequisites that are features discussed below, are probably incomplete and more will have to be added in the near future.

If the program indicates numerical or structural chromosomal abnormalities, the operator wants to be sure that the observed abnormalities are real and not false positive artifacts. A poorly labeled probe or a probe that has not hybridized efficiently would result in such a false positive result. Without graphs that show the fluorescence intensity values for each probe, such as that shown in figure 4, it would be difficult to detect such an error. Chromosome by chromosome quality control evaluation capability is essential.

The user needs a simple means to confirm chromosome identity. This should not only be based on a color code. Figure 6 shows that in cases where extensive chromosome rearrangements occur the color code becomes very difficult to interpret and thus does not yield the desired information any more. Our software is capable of displaying individual chromosomes or chromosome segments identified in the fluor masks on the basis of their fluor composition on the computer monitor next to the DAPI image. In our opinion, these black and white representations of individual chromosome material next to the DAPI image in addition to the 'stick models' shown in figures 6(*c*) and (*f*) yield the highest degree of information. They do not look very spectacular but facilitate an accurate diagnosis tremendously. Thus, we believe that the future of multicolor techniques is 'black and white'.

4.5. Usefulness of M-FISH

M-FISH will be useful for a broad range of applications from karyotyping to the three-dimensional elucidation of the organization of the genome in intact interphase nuclei (for reviews see LeBeau 1996, Speicher and Ward 1996). Future developments will include: the incorporation of additional fluors to expand the combinatorial labeling capacity, the simultaneous use of fluorescence banding techniques for regional chromosomal identification and correlation studies with conventional cytogenetic methods, the development of specific diagnostic probe sets for detecting cryptic translocations and identifying specific chromosomal translocations in leukemias and lymphomas, and three-dimensional image algorithms for analysing the organization of genomic DNA in intact interphase nuclei as a function of developments and differentiation.

Acknowledgments

We thank Nurit Mokady for propagating the cell lines. This work was supported by grant 93-018 from the Department of the Army. MRS was the recipient of a grant from the Deutsche Forschungsgemeinschaft (Sp 460/1-1).

References

Bauman J GJ, Pinkel D, Trask B and van der Ploeg M 1989 Flow cytometric measurement of specific DNA and RNA sequences. *Flow Cytogenetics* (New York:Academic) pp 275–301

Dauwerse J G, Wiegant J, Raap A K, Breuning M H and van Ommen G J B 1992 Multiple colors by fluorescence *in situ* hybridization using ratio-labelled DNA probes create a molecular karyotype *Hum. Mol. Genet.* **1** 593–8

du Manoir S, Schröck E, Bentz M, Speicher M R, Joos S, Ried T, Lichter P and Cremer T 1995 Quantitative analysis of comparative genomic hybridization *Cytometry* **19** 27–41

du Manoir S, Speicher M R, Joos S, Schröck E, Popp S, Döhner H, Kovacs G, Robert-Nicoud M, Lichter P and Cremer T 1993 Detection of complete and partial chromosome gains and losses by comparative genomic *in situ* hybridization *Hum. Genet.* **90** 590–610

Ernst L A, Gupta R K, Mujumdar R B and Waggoner A S 1989 Cyanine dye labeling reagents for sulfhydryl groups *Cytometry* (bf)10 3–10

Guan X Y, Meltzer P S, Burgess A and Trent J M 1995 Complete coverage of chromosome 6 by chromosome microdissection: Generation of 14 band region-specific probes *Hum. Genet.* **95** 637–40

Guan X Y, Meltzer P S and Trent J M 1994 Rapid generation of whole chromosome painting probes (WCPs) by chromosome microdissection *Genomics* (bf)22 101–7

Guan X Y, Trent J M and Meltzer P S 1993 Generation of band-specific painting probes from a single microdissected chromosome *Hum. Mol. Genet.* **2** 1117–21

Guan X Y, Zhang H, Bittner M, Jiang Y, Meltzer P and Trent J 1996 Chromosome arm painting probes *Nature Genet.* **12** 10–1

Kallioniemi A, Kallioniemi O P, Sudar D, Rutovitz D, Gray JW, Waldman F and Pinkel D 1992 Comparative genomic

hybridization for molecular cytogenetic analysis of solid tumors *Science* **258** 818–21

LeBeau M M 1996 One FISH, two FISH, red FISH, blue FISH *Nature Genet.* **12** 341–4

Ledbetter D H 1992 The 'colorizing' of cytogenetics: is it ready for prime time? *Hum. Mol. Genet.* **5** 297–9

Lengauer C, Speicher M R, Popp S, Jauch A, Taniwaki M, Nagaraja R, Riethman H C, Donis-Keller H, d'Urso M, Schlessinger D and Cremer T 1993 Chromosomal bar codes constructed by fluorescence *in situ* hybridization with Alu-PCR products of multiple YAC clones *Hum. Mol. Genet.* **2** 505–12

Meltzer P S, Guan X Y, Burgess A and Trent J 1992 Rapid generation of region specific probes by chromosome microdissection and their application *Nature Genet.* **1** 24–8

Mujumdar R B, Ernst L A, Mujumbar S R and Waggoner A S 1989 Cyanine dye labeling reagents containing isothiocyanate groups *Cytometry* **10** 11–19

Nederlof P M, Robinson D, Abuknesha R, Wiegant J, Hopman A HN, Tanke H J and Raap A K 1989 Three color fluorescence *in situ* hybridization for the simultaneous detection of multiple nucleic acid sequences *Cytometry* **10** 20–7

Nederlof P M, van der Flier S, Vrolijk J, Tanke H J and Raap AK 1992 Fluorescence ratio measurements of double-labeled probes for multiple *in situ* hybridization by digital imaging microscopy *Cytometry* **13** 839–45

Nederlof P M, van der Flier S, Wiegant J, Raap A K, Tanke HJ, Ploem J S and van der Ploeg M 1990 Multiple fluorescence *in situ* hybridization *Cytometry* **11** 126–31

Piper J, Rutovitz D, Sudar D, Kallioniemi A, Kallioniemi OP, Waldman F M, Gray J W and Pinkel D 1995 Computer image analysis of comparative genomic hybridization *Cytometry* **19** 10–26

Popp S, Jauch A, Schindler D, Speicher M R, Lengauer C, Donis-Keller H, Riethman H C and Cremer T 1993 A strategy for the characterization of minute chromosome rearrangements using multiple color fluorescence *in situ* hybridization with chromosome specific DNA libraries and YAC clones *Hum. Genet.* **92** 527–32

Ried T, Baldini A, Rand T C and Ward D C 1992a Simultaneous visualization of seven different DNA probes by *in situ* hybridization using combinatorial fluorescence and digital imaging microscopy *Proc. Natl Acad. Sci. USA* **89** 1388–92

Ried T, Landes G, Dackowski W, Klinger K and Ward D C 1992b Multicolor fluorescence *in situ* hybridization for the simultaneous detection of probe sets for chromosomes 13, 18, 21, X and Y in uncultured amniotic fluid cells *Hum. Mol. Genet.* **1** 307–13

Schrock E, du Manoir S, Veldman T, Schoell B, Wienberg J, Ferguson-Smith M A, Ning Y, Ledbetter D H, Bar-AM I, Soenksen D, Garini Y and Ried T 1996 Multicolor spectral karyotyping of human chromosomes *Science* **273** 494–7

Smith T G Jr, Marks W B, Lange G D, Sheriff W H Jr and Neale E A 1988 Edge detection in images using Marr–Hildreth filtering techniques *J. Neurosci. Meth.* **26** 75–81

Speicher M R, Ballard S G and Ward D C 1996 Karyotyping human chromosomes by combinatorial multi-fluor FISH *Nature Genet.* **12** 368–75

Speicher M R, Howe C, Crotty P, du Manoir S, Costa J and Ward D C 1995 Comparative genomic hybridization detects novel deletions and amplifications in head and neck squamous cell carcinomas *Cancer Res.* **55** 1010–13

Speicher M R and Ward D C 1996 The coloring of cytogenetics *Nature Med.* **2** 1046–48

Trask B, van den Engh G, Pinkel D, Mullikin J, Waldman F, van Dekken H and Gray J 1988 Fluorescence *in situ* hybridization to interphase cell nuclei in suspension allows flow cytometric analysis of chromosome content and microscopic analysis of nuclear organization *Hum. Genet.* **78** 251–9

Waggoner A 1995 Covalent labeling of proteins and nucleic acids with fluorophores *Meth. Enzymology* **246** 362–73

Waggoner A, Debasio R, Conrad P, Bright G R, Ernst L, Ryan K, Nederlof M and Taylor D 1989 Multiple spectral parameter imaging *Meth. Cell. Biol.* **30** 449–78

Wiegant J, Wiesmeijer C C, Hoovers J M, Schuuring E, d'Azzo A, Vrolijk J Tanke H J and Raap A K 1993 Multiple and sensitive fluorescence *in situ* hybridization with rhodamine-, fluorescein-, and coumarin-labeled DNAs *Cytogenet. Cell Genet.* **63** 73–6

Yu H, Chao J, Patek D, Mujumdar R, Mujumdar S and Waggoner A S 1994 Cyanine dye dUTP analogs for enzymatic labeling of DNA probes *Nulc. Acids Res* **22** 3226–32